UNIVERSITY OF CALIFORNIA, SAN DIEGO

Functional Mapping of Auto-Inhibitory Sites in Talin

A dissertation submitted in partial satisfaction of the
requirements of the degree Doctor of Philosophy

in

Molecular Pathology

by

Asoka Banno

Committee in charge:

Professor Mark H. Ginsberg, Chair
Professor Jack E. Dixon
Professor Sanford J. Shattil
Professor Dwayne G. Stupack
Professor Susan S. Taylor

2011

The Dissertation of Asoka Banno is approved, and it is acceptable in quality and form for publication on microfilm and electronically:

_____

_____

_____

_____

_____

Chair

University of California, San Diego

2011

Dedication

in memory of

Mia Mia

who is my happiness

and has forever changed my life

Epigraph

世の中の人は何とも言わば言え、

我が成すことは我のみぞ知る。

坂本竜馬

Table of Contents

List of Abbreviations

aa	amino acid(s)
ADP	adenosine diphosphate
Avi	avidin
BMRB	BioMagResBank
CalDAG-GEF1	Ca^{2+}- and DAG-regulated guanine nucleotide exchange factor 1
CD	cluster of differentiation
cDNA	complementary deoxyribonucleic acid
CHO	Chinese hamster ovary
CIB	calcium- and integrin-binding protein
C-terminal	carboxyl-terminal
DMPC	1,2-dimyristoyl-*sn*-glycero-3-phosphocholine
DMPG	1,2-dimyristoyl-*sn*-glycero-3-phospho-(1'rac-glycerol)
DOK-1	docking protein 1
DTT	dithiothreitol
ECL	enhanced chemiluminescence
ECM	extracellular matrix
EDTA	ethylenediaminetetraacetic acid
ER	endoplasmic reticulum
ERK1/2	extracellular signal-regulated kinases 1 and 2
FERM	4.1-ezrin-radixin-moesin

FL	full-length
FRET	Förster resonance energy transfer
GDP	guanosine diphosphate
GEF	guanine exchange factor
GFP	green fluorescent protein
GP	glycoprotein
GST	glutathione *S*-transferase
GTP	guanosine triphosphate
HA	hemagglutinin
HEPES	4-(2-hydroxyethyl)-1-piperazineethanesulfonic acid
His	Histidine
HSQC	heteronuclear single quantum coherence
HPLC	high performance (pressure) liquid chromatography
H-Ras	Harvey-Ras
HRP	horseradish peroxidase
iC3b	inactive complement factor 3b fragment
ICAM	inter-cellular adhesion molecule
ICAP-1	integrin cytoplasmic domain-associated protein 1
Ig	immunoglobulin
LAD	leukocyte adhesion deficiency
LAMP1	lysosome-associated membrane protein 1
LIBS	ligand-induced binding site

MAP kinase	mitogen-activated protein kinase
MD	membrane-distal
MFI	median fluorescence intensity
MOP	membrane orientation patch
MP	membrane-proximal
MSP	membrane scaffold protein
Myc	myelocytomatosis
NMR	nuclear magnetic resonance
NORE1B	novel ras effector 1B
N-terminal	amino-terminal
PAGE	polyacrylamide gel electrophoresis
PBS	phosphate buffered saline
PCR	polymerase chain reaction
PH	pleckstrin homology
PI3K	phosphatidylinositol 3- kinase
PIP2	phosphatidylinositol 4,5-biphosphate
PIPES	piperazine-N,N′-bis-(2-ethanesulfonic acid)
PIPKIγ-90	phosphatidylinositol phosphate kinase type Iγ-90
PMSF	phenylmethylsulfonyl fluoride
PTB	phosphotyrosine-binding
Rap	Ras-related protein
Ras	rat sarcoma

RapL	regulator for cell adhesion and polarization enriched in lymphoid tissues
RhoGDI	Rho protein GDP-dissociation inhibitor
RIAM	Rap1-GTP interacting adaptor molecule
R-Ras	related-Ras
Scr	scramble
SDS	sodium dodecyl sulfate
SE	standard error
Src	sarcoma
TBS	tris buffered saline
THD	talin head domain
TM	transmembrane
VBS	vinculin binding site
WT	wild type

List of Figures

List of Tables

Acknowledgments

I would like to thank Dr. Mark H. Ginsberg for his guidance throughout my thesis research. By sharing his wisdom in science and by providing a great environment full of outstanding scientists, he has made my five years as a graduate student a truly learning experience.

I would also like to acknowledge the Ginsberg lab members for their support and advice and for creating a cheerful "home" for me. Especially, I am grateful to Feng Ye, Jake R. Haling, Brian G. Petrich, Wilma Puzon-McLaughlin, and Li-Ting Su. Through our daily interactions, Feng has demonstrated what it takes to be a good scientist and has become the person that I look up to. In addition to giving me invaluable advice and support, he helped me overcome frequent roadblocks. If it were not for Jake having paved the way of a graduate student in the Ginsberg lab before me, I would have had a more difficult time in the lab. I would like to thank Brian for taking the time to read and edit my dissertation and giving me insightful suggestions. I am grateful to Wilma who welcomed me into the lab on my memorable, first day in the Ginsberg lab. It was Wilma who taught me how to clone and how to use flow cytometry, two major techniques that I have used throughout my graduate studies. She is also an excellent lab manager who makes our work run smoothly. Li-Ting, through her friendship, gave me a chance to breath in between experiments and made the last few stressful months bearable for me.

I would like to thank my committee, Dr. Jack E. Dixon, Dr. Sanford J. Shattil, Dr. Dwayne G. Stupack, and Dr. Susan S. Taylor. Their advice guided my research in the right direction.

I would like to thank my parents and my sister. If it were not for my parents' confidence in me and their respect for my decision 15 years ago, my life would not be where it is today. No one is better at making me laugh than Akari. Especially during the last five years, I have come to cherish the time spent with her as my brief vacation from science. I also appreciate her willingness to forgive her difficult sister.

I would like to give special thanks to Scott A. Stuart for his constant support. I would not have survived this far if it were not for his knowledge and experience as a scientist and his understanding and encouragement as a friend. Over the last five years, he has become a resourceful mentor and an irreplaceable friend for me.

Finally, I would like to acknowledge MiaMia who has always been there for me and has never given up on me. I am indebted to her for my happiness.

The texts of Chapters 1 through 4, in part, are being prepared for publication. Asoka Banno, Benjamin T. Goult, Feng Ye, David R. Critchley, Mark H. Ginsberg. "Functional Mapping of Auto-Inhibitory Sites in Talin". I was the primary investigator of this research as well as the primary author of the manuscript.

Vita

Education

Doctor of Philosophy in Molecular Pathology
University of California, San Diego, CA 2006-2011

Bachelor of Science in Biology, *cum laude*
American University, Washington, D.C. 1998-2001

Publications

Kahner, B. N., Ye, F., Kato, H., **Banno, A.**, Ginsberg, M. H., and Shattil, S. J. (2011) "Pinpointing the Locus of Action of Kindlins in Integrin αIIbβ3 Activation", submitted to *J Biol Chem*

Banno, A., and Ginsberg, M. H. (2008) "The Ins and Outs of Integrin Signaling", in *Cell Junctions: Adhesion, Development and Disease*, edited by LaFlamme, S. E. and Kowalczyk, A. P. Wiley-VCH, Germany

Banno, A., and Ginsberg, M. H. (2008) *Biochem Soc Trans* **36**, 229-234

Minami, Y., Stuart, S. A., Ikawa, T., Jiang, Y., **Banno, A**., Hunton, I. C., Young, D. J., Naoe, T., Murre, C., Jamieson, C. H., and Wang, J. Y. (2008) *Proc Natl Acad Sci U S A* **105**, 17967-17972

Nunez Rodriguez, N., Lee, I. N., **Banno, A**., Qiao, H. F., Qiao, R. F., Yao, Z., Hoang, T., Kimmelman, A. C., and Chan, A. M. (2006) *Mol Cell Biol* **26**, 7145-7154

Narla, G., DiFeo, A., Yao, S., **Banno, A**., Hod, E., Reeves, H. L., Qiao, R. F., Camacho-Vanegas, O., Levine, A., Kirschenbaum, A., Chan, A. M., Friedman, S. L., and Martignetti, J. A. (2005) *Cancer Res* **65**, 5761-5768

Kimmelman, A. C., Qiao, R. F., Narla, G., **Banno, A**., Lau, N., Bos, P. D., Nunez Rodriguez, N., Liang, B. C., Guha, A., Martignetti, J. A., Friedman, S. L., and Chan, A. M. (2004) *Oncogene* **23**, 5077-5083

Honors, Awards, and Fellowships

Tobacco-Related Disease Research Program Dissertation Research Award
University of California 2008-2010

Graduated *cum laude*
American University 2001

Golden Key National Honor Society Membership 2001-present

National Dean's List 2001

Early Identification Program Membership
(for academically outstanding students with a GPA 3.7 or higher)
American University 1999

Dean's List for Superior Academic Performance
American University 1999-2001

Research Experiences

Research Associate for Dr. Jean Wang
University of California, San Diego, CA 2005-2006
- Development of CML/BCR-ABL mouse model
- Development of an *in-vitro* system for the analysis of Reactive Oxygen Species (ROS) production in CML
- Examination of BCR-ABL-induced ROS production
- Investigation of the relationship between ß-catenin and BCR-ABL

Assistant Researcher for Dr. Andrew Chan
Mount Sinai School of Medicine, NY 2003-2005
- Investigation of the role of R-Ras in tumor progression/metastasis
- Examination of the relationship between R-Ras and integrin expression in metastatic tumors
- Characterization and biological analysis of tumor cells by invasion/migration, adhesion, and cell proliferation assays
- Assistance in identification and characterization of a tumor suppressor, KLF6, in glioblastoma

QC Technician II
Orchid Diagnostics, CT 2001-2003
- QC testing of raw materials, intermediates, and final products
- Maintenance of detailed records and documents of all the experiments
- Investigation and trouble-shooting of customer complaints
- Assistance in product development

ABSTRACT OF THE DISSERTATION

Functional Mapping of Auto-Inhibitory Sites in Talin

by

Asoka Banno

Doctor of Philosophy in Molecular Pathology

University of California, San Diego, 2011

Professor Mark H. Ginsberg, Chair

Integrin activation by 'inside-out' signaling is a key process in cell migration and adhesion to extracellular matrix. Recent *in-vivo* and *in-vitro* studies have provided convincing evidence that the binding of talin, a cytoskeletal protein, to the integrin β cytoplasmic tails is necessary and sufficient for integrin activation. The significance of its role in integrin signaling leads to the expectation that functions of talin are tightly controlled. Indeed, previous data have shown that cellular distribution of talin and its interaction with integrins is highly regulated; talin resides in the cytosol

of platelets under resting conditions but, in response to intracellular signals, translocates to the membrane where it interacts with and activate integrins. However, despite intense interests and vigorous efforts, our understanding of molecular basis of talin regulation remains incomplete.

In contrast to FL talin, the N-terminal THD binds to and strongly activates integrins without requiring additional signaling. Thus, we hypothesized that a region in the talin rod domain is involved in suppressing the functions of talin. Sequential C-terminal truncations of the talin rod domain and subsequent mutational analysis revealed that an α-helical bundle termed Domain E negatively regulates membrane recruitment of talin via its inter-domain interaction with the F3 domain of talin. However, increased membrane association of talin caused by disruption of the Domain E-F3 interaction is insufficient for plasma membrane localization of talin, for the talin-integrin interaction, or for integrin activation in cells or in an *in-vitro* nanodisc system. NMR analysis revealed an inter-domain interaction between another α-helical bundle in the talin rod called VBS1/2a and the F23 domain of talin, and truncation of VBS1/2a led to increased plasma membrane localization of talin. In addition, truncation analysis identified a short fragment within the linker region between THD and the rod domain that interferes with the talin-integrin interaction. In this study, we

have mapped three auto-inhibitory sites within talin and have assigned a specific function to each one of them. These findings provide insights as to how talin is regulated and what may happen to talin during the final steps in integrin activation.

Chapter 1:

Introduction

Integrin Overview

Integrins are a family of adhesion receptors found in metazoans, from the simplest sponges and cnidaria to the most complex mammals (1). They function as glycosylated heterodimers composed of non-covalently associated type I transmembrane (TM) α and β subunits (2). Each integrin subunit contains a large extracellular domain (>700 amino acids (aa)), a single TM domain (>20 aa), and a generally short cytoplasmic domain (13-70 aa) (3). Integrin TM domains are believed to begin after an extracellular Pro residue (3). In contrast, the boundary between the TM and the cytoplasmic domains is less clear. Nevertheless, the membrane-proximal (MP) regions of the cytoplasmic tails are conserved in most human integrin α and β subunits, starting with a conserved Lys/Arg residue followed by GFFKR in the α subunit and LLxxxHDRRE in the β subunit, leading many to assume that the cytoplasmic domains begin at the conserved Lys/Arg residue (4).

In humans 18 α and 8 β subunits form at least 24 different heterodimers. In general, each of the 24 integrins has a distinct, non-redundant function, binding to a specific repertoire of cell surface, extracellular matrix (ECM), and soluble protein ligands (1). Specificity of integrin function is mainly determined by the combination of α and β subunits, by the cellular repertoire of integrins expressed, by the functional state of those integrins, and by the availability of specific integrin ligands (1,2).

Furthermore, cell-type specific expression of integrins and alternative splicing of extracellular and cytoplasmic domains add to the potential complexity of integrin function (2,5).

During the 25 years since the recognition of the integrin family and the introduction of the term 'integrin', extensive study has greatly furthered our understanding of these adhesion receptors (6,7). Playing central roles in cell migration and cell-ECM adhesion and controlling cell differentiation, proliferation, and apoptosis, integrins are essential contributors in development, immune responses, hemostasis, and numerous human diseases such as cancer and autoimmune diseases (1).

Cell attachment and responses to ECM are important requirements for development of multicellular organisms, and here integrins serve as TM mechanical links between the ECM outside of a cell and the cytoskeleton inside of the cell (1,8). Integrin-ECM interaction leads to occupancy and clustering of integrins, which in turn promotes recruitment of cytoskeletal and cytoplasmic proteins such as talin, paxillin, and α-actinin to form focal complexes and focal adhesions (2). Within these dynamic adhesion complexes, the cytoplasmic domains of the clustered integrins recruit cytoskeletal proteins and signaling molecules into a close proximity at high concentrations, enabling integrins to initiate intracellular signaling cascades. These signaling events initiated upon integrin occupancy, which are referred to as 'outside-in' integrin signaling, enable integrins to regulate a variety of cellular behaviors, including cell migration, differentiation, proliferation, and apoptosis (1,9,10).

As an integral part of the plasma membrane, connecting the cytoskeleton to ECM, integrins also play a role in mechanotransduction and mediate the transmission of mechanical stress across the plasma membrane (11,12). They are also capable of transducing physical forces into cellular chemical signals, with a help of other signaling molecules that co-localize in focal adhesions (11,13). For instance, changes in the balance of forces across integrins and the resulting alteration in cell shape can modulate growth, differentiation, and apoptosis (12).

Integrin Activation

Integrins are in equilibrium between low and high affinity states under physiological conditions. However, many integrins are expressed and remain in the low affinity binding state for their ligands until cellular stimulation transforms them into a high affinity form (1). This regulation of cell adhesion by signals from within the cell is called 'inside-out' signaling (14,15), and the rapid process of shifting from the low to high affinity states is often defined as 'integrin activation' (1,3,5). Here, the term 'activation' refers to the transition to the high affinity state, an event that is accomplished by the propagation of conformational changes from the integrin cytoplasmic domain to the extracellular domain (16-18). This process of activation that leads to integrin occupancy and clustering (2) should not be confused with the interactions of integrins with extracellular ligands that initiate signaling events into the cell as in integrin 'outside-in' signaling (19) .

Activation and inactivation of integrins is tightly regulated. Although not all integrins have been shown to undergo extremes of activity, it is generally believed that most integrins shift between active and inactive states in a localized fashion when it is important for cells to regulate their adhesion in a temporal and spatial manner (1,5,19). The importance of integrin activation is well demonstrated in the functions of platelets and leukocytes (1,5).

αIIbβ3 integrins, also known as GPIIb-IIIa, are present at high density on resting circulating platelets but remain inactive under normal conditions (1,5). Upon platelet stimulation by agonists such as thrombin, ADP, or epinephrine acting through G protein-coupled receptors, by von Willebrand factor signaling through its receptor (GPIb/V/IX), or by collagen binding to its receptor GPVI, signals from within the cell activate αIIbβ3 integrin to bind to ligands such as fibrinogen, von Willebrand factor, and fibronectin (1,5). Binding of these multivalent ligands to activated αIIbβ3 leads to platelet aggregation. It is crucial that αIIbβ3 is inactive on resting circulating platelets, for constitutive or deregulated αIIbβ3 integrin activation causes unregulated platelet aggregation, leading to thrombosis (1,5). In contrast, defects in or lack of αIIbβ3 integrins result in defects in hemostasis seen in the bleeding disorder called Glanzmann's thrombasthenia (1).

In a very similar fashion to αIIbβ3 integrins on platelets, the β2 integrins, also known as CD11/18, on leukocytes are precisely regulated (1,5). They are expressed in their resting state on most white blood cells. When the cells encounter agonists such as chemokines, the β2 integrins become rapidly activated to mediate firm adhesion to

their ligands that include counter-receptors such as Ig superfamily molecules (*e.g.* ICAM-1, 2, and 3), ECM proteins (*e.g.* fibronectin), blood clotting proteins such as fibrinogen, and the complement pathway product, iC3b (1,20,21). For instance, the β2 integrins interact with ICAMs, major ligands of the β2 integrins, to mediate processes such as phagocytosis, cytotoxic killing, and efficient antigen presentation (1,20). As in the case of αIIbβ3 integrins on platelets, it is critical that the β2 integrins remain inactive on resting leukocytes, for their deregulated activation or impaired de-activation causes failure in normal immune responses (22). Similarly, lack of or dysfunction in rapid activation of the β2 integrins leads to defective immune function seen in patients with leukocyte adhesion deficiency (LAD) who suffer from leukocytosis and the failure to recruit leukocytes to the sites of infection (1,5).

As noted above, integrin activation is primarily the result of conformational changes that are initiated at the cytoplasmic face of the integrins and propagated to the extracellular domains. Several key advances have provided important insights as to what takes place at each step in the activation process and how conformational changes may travel from the cytoplasmic to the extracellular domains through the plasma membrane.

Since the crystal structure of the extracellular domain of αVβ3 integrin was solved 10 years ago (23), much understanding of integrin structure and function has been achieved (24-26). Based on studies using a variety of methods, extracellular domains of integrins appear to assume at least three conformations; a bent "closed" conformation, an intermediate extended conformation with a closed headpiece, and an

extended "open" conformation (23,27,28). They may represent low affinity, activated, and activated and ligand-bound states of integrins, respectively (27-31). However, the bent form can bind ligands with high affinity (32) in some circumstances, which has led to the proposition of an alternative 'deadbolt' model for 'inside-out' activation, emphasizing that an extended conformation is not necessary for integrins to bind to their physiological ligands (32,33). The discrepancies between studies are most likely due to the differences in methodology as well as to the fact that the conformations of integrins have been studied in isolated extracellular domains or in fragments (34). Thus, resolution of the global rearrangements in integrin conformation accompanying 'inside-out' signaling will require structural analysis of a full-length integrin in a physiological context.

In addition to modulation of integrin affinity via conformational change within a single receptor molecule (affinity modulation), increased integrin-mediated adhesion can also be caused by receptor clustering on the cell surface (avidity modulation) (35-38). Furthermore, in most circumstances, it is likely that some combination of conformational change and receptor clustering is involved in regulation of integrin-mediated adhesion. In one insightful report, a monovalent antibody and a conditional dimerizer were used to isolate the relative contributions of affinity modulation and receptor clustering in αIIbβ3-meditated functions (39). In particular, this work showed that affinity modulation and avidity modulation play complementary roles in the adhesive functions of this integrin.

The TM domains of integrins are highly conserved amongst each of the α and the β subunits and are also conserved between species (40). Mutations in the TM region can lead to loss of integrin expression (41-43), which strongly suggests their essential role in integrin functions. Integrin activation, which is accompanied by conformational rearrangements transmitted from the cytoplasmic to extracellular domains, must certainly involve alteration of the TM domain in this signal transduction process. Indeed, recent studies have begun to provide insights into how rearrangements within the TM domain can lead to integrin activation.

Helical packing of integrin TM regions is likely to depend on specific crossing angles and specific in-register side chain arrays (44). A recent NMR analysis showed that, in the αIIbβ3 TM complex corresponding to the resting state, the αIIb helix is perpendicular to the membrane and that the β3 helix is tilted by approximately 25° (45). Furthermore, another study using an affinity capture assay in combination with NMR revealed specific interactions between the αIIb and the β3 TM domains and demonstrated the importance of these interactions in integrin activation (46). Within the membrane, the α and the β subunits form two contacts: an 'inner membrane clasp' and an 'outer membrane clasp' (45). The 'outer membrane clasp' is formed by the close helical packing mediated by Gly residues, whereas the 'inner membrane clasp' is stabilized by a salt bridge between Arg995 of the αIIb and Asp723 of the β3 subunits (45). Indeed, an electrostatic interaction was proposed to stabilize the inactive conformation of integrins 15 years ago (16). These two clasps together stabilize the

TM complex, and mutations that disrupt either one destabilize the association between the αIIb and the β3 TM domains (45,46).

Mutational analysis together with computational molecular modeling together have suggested that the α and β subunit TM complex stabilizes the inactive state of integrins and that its disruption results in integrin activation (41,44,47-49). However, some activating mutations may weaken but not completely separate the TM complex (45,46). Therefore, questions still remain as to whether the separation of the TM domains is indeed coupled to the conformational state of the extracellular domains. Likewise, alternative models for the rearrangements in TM domains, *i.e.* pistoning, twisting, and hinging, remain plausible (4).

The cytoplasmic face of the integrins is where integrin 'inside-out' signaling begins, therefore, needless to say, changes in interactions and/or in the structures of the cytoplasmic domains of integrins within the highly-conserved regions play crucial roles in integrin activation via 'inside-out' signaling (3,4,50,51). Indeed, there is direct experimental evidence for a change in the relationship of the integrin α and β cytoplasmic domains during integrin activation (52).

The MP regions of the α and the β tails are believed to interact in part through the above-mentioned salt bridge between the conserved Arg995 of αIIb and Asp723 of β3 subunits, respectively, (or between the corresponding residues in other integrins) and the hydrophobic residues immediately N-terminal to them (16,51,53,54). Together with the TM complex, this specific association forming a 'clasp' between the α and the β subunits is thought to prevent integrin activation by stabilizing the low

affinity state (16). In support of this, mutations that disrupt this 'clasp' lead to integrin activation (15,16,51,54). Integrins can also be constitutively activated by deletion of the entire α cytoplasmic tail or of the MP GFFKR sequence (15,16,51,54). Likewise, deletion of or certain point mutations in the MP region of the β tail result in integrin activation (16,51,55). Furthermore, replacement of the cytoplasmic-TM regions by heterodimeric coiled-coil peptides or an artificial linkage of the tails inactivates the receptor, and breakage of the coiled-coil or clasp activates integrins (55-57). These data together strongly indicate that hydrophobic and electrostatic interactions stabilize the association between the α and the β MP regions, thereby maintaining the integrins in a low affinity state. The importance of the α and β tail interaction is further supported by a study using FRET; in the resting state, fluorophore tagged α and β tails were close enough to undergo FRET, however stimulation with agonists or introduction of activating mutations to the MP region of the α subunit led to a reduction in FRET (58). The reduction in FRET was interpreted as separation of the cytoplasmic domains, although it could possibly be due to an alteration in orientation of the α and the β cytoplasmic tails relative to each other without changing the distance between the cytoplasmic domains (58,59).

In contrast to the effects of deletion of or mutations in the MP region of the β cytoplasmic tails, deletion of or mutations in the β tails that are further C-terminal, *i.e.* the membrane-distal (MD) region, block integrin activation. In particular, an NPxY/F motif of the β subunit has been identified as one of the critical sites (54,60). Tyr/Phe-to-Ala mutation in this conserved motif blocks integrin activation (61). Importantly,

physiological integrin activation process also requires the MD region of the β3 cytoplasmic domain (62). We now know, as further discussed below, that mutations in the NPxY motif perturb the binding of integrin β tails to numerous cytoskeletal and signaling protein (63), thus accounting for their profound effects on integrin signaling.

In summary, structural and mutational analyses combined with molecular modeling of the past decade have demonstrated how intracellular signals and the consequent conformational changes propagate from the cytoplasmic to the extracellular domains and result in integrin activation. Our current model illustrates that cellular stimulation triggers the release of the structural constraints and the rearrangement in the cytoplasmic domains. These intracellular events then travel across the plasma membrane as the rearrangements in the α-β TM complex and initiate the conformational changes in the extracellular domains, finally leading to integrin activation.

Regulation of Integrin Activation

Although 'inside-out' signaling can also be achieved via affinity-independent mechanisms such as changes in integrin diffusion and integrin clustering, a major focus of the integrin research over the past decade has been on affinity-dependent regulation of integrin-mediated adhesion (1,3,5,9). Efforts at deciphering the mechanism of this form of integrin signaling have produced compelling evidence that the integrin cytoplasmic domains are the targets of intracellular signals that modulate ligand binding affinity (15,54,63).

Analysis of the integrin 'adhesome' has identified a network of at least 156 proteins that are linked by numerous protein-protein interactions (64). Some of these are adaptor proteins that assemble various components in a spatially- and temporally-specific manner, whereas others are signaling proteins with enzymatic activities such as kinases and phosphatases.

Among the core members of the 'adhesome', more than 19 proteins bind directly to the integrin β cytoplasmic tails (64). Some of these β tail-binding proteins, including talin (65,66), β3-endonexin (67-69) and cytohesins-1 and -3 (70,71), induce integrin activation. Others such as CIB (72), paxillin (73), and RapL (also known as NORE1B) (74,75) are implicated in the regulation of integrin activation by associating with the integrin α subunit. However, the significance of many of these interactions in physiological context has yet to be verified (50). One exception is talin; talin is now widely accepted as the critical player in integrin activation and will be discussed further in detail as the focus of this study. In addition to talin, recent studies have also highlighted the kindlin family of proteins as important contributors to integrin activation (76). Yet other proteins, *e.g.* DOK-1 (77), ICAP-1 (78), and filamin (79), may regulate integrin activation by competing with talin for the integrin β tails (50,80,81).

Signaling proteins also influence integrin activation, even when they do not directly interact with integrin cytoplasmic tails. For example, Hughes, P.E. *et al*. found that H-Ras and its downstream effector kinase, Raf-1, suppress integrin activation in Chinese hamster ovary (CHO) cells via activation of the ERK1/2-MAP

kinase pathway, independently of *de novo* protein synthesis or integrin phosphorylation (82,83). However, this suppression of integrin affinity by H-Ras is cell-type specific; in contrast to CHO cells and fibroblasts, H-Ras can promote integrin activation in other cell types such as certain hematopoietic cell lines (82). In contrast, R-Ras, another small GTPase that shares many common effectors with other Ras family members, generally activates integrins (84,85). Expression of a constitutively active variant of R-Ras converted two suspension cell lines into highly adherent cells, whereas introduction of a dominant negative form of R-Ras reduced the adhesiveness of CHO cells (85). Cell-type specificity of integrin affinity regulation by these signaling pathways is probably due to variations in expression of these GTPases or of the upstream and/or downstream elements that link them to integrin activation (86).

Recent studies have identified Rap GTPase as a potent activator of integrins that is capable of inducing cell adhesion independent of PI3K (82,87,88). In fact, many cytokines and growth factors promote integrin-dependent cell adhesion through the activation of Rap, and this is true with various subtypes of integrins in various cellular contexts (82). Furthermore, Rap1 is now known to regulate all of the integrins that are associated with actin cytoskeleton, *i.e.* integrins of the β1, β2, and β3 family (89). In patients with LAD-III who suffer from defects in leukocyte and platelet integrin activation, the β1, β2, and β3 integrins are not mutated and are expressed at normal levels. Yet, cells from these patients are impaired in their abilities to bind to integrin ligands with high affinity in response to chemoattractant signals (90,91).

While expression of Rap1 and talin appears normal in these patients, an autosomal recessive mutation in CalDAG-GEFI, a key Rap1/2 GEF, (90) is associated with LADIII. Consistent with this observation, *CalDAG-GEFI*$^{-/-}$ mice exhibit defects in activation of Rap1 as well as of the β1, β2, and β3 integrins and therefore impaired inflammatory response and lack of thrombus formation (91). Thus, Rap1 and CalDAG-GEFI are critical regulators of inside-out integrin activation in human T lymphocytes, neutrophils, and platelets (90,91).

In the past several years, RIAM has emerged as a key molecule involved in Rap1-induced integrin-mediated cell adhesion and cell spreading (89,92). Overexpression of RIAM induced the active conformation of integrins and enhanced cell adhesion while knocking down RIAM eliminated adhesion mediated by Rap1 (92). Furthermore, a study that reconstructed a synthetic integrin activation pathway in CHO cells has identified an 'integrin activation complex' consisting of active Rap1, RIAM, and talin, the formation of which ultimately leads to talin binding to the integrin β cytoplasmic tail and thereby to integrin activation (86). The critical role that RIAM plays in the regulation of integrin activation will be discussed further below.

Talin

Talin was the first cytoplasmic protein shown to bind directly to integrins (66). Over the 25 years since this discovery, the finding has been confirmed for β1 (65), β2 (93), and β3 (65) integrins. More recent studies have established the talin-integrin

interaction as a final, common step in activation of several classes of integrins (65,94,95). Furthermore, both *in-vivo* (96-98) and *in-vitro* (65,95,99) studies have convincingly shown that the binding of talin to the integrin β cytoplasmic tails is necessary and sufficient for integrin activation.

Talin, a name derived from a Latin word 'talus' for ankle because of its prominent location in adhesion plaques (100,101), is a major cytoskeletal protein that colocalizes with activated integrins, actin, and actin-binding proteins such as vinculin (102,103). Two isoforms are found in vertebrates; talin 1 is ubiquitously expressed, whereas talin 2 is expressed primarily in striated muscle and in the brain (104). This study was focused on talin 1. Talin 1 is a 2541 amino acid protein, consisting of an N-terminal globular head domain of ~50kDa and a C-terminal rod domain of ~220kDa (105). Talin head domain (THD) contains an F0 domain and a FERM domain that can be divided into three subdomains, F1, F2, and F3. FERM domains often mediate interactions with the cytoplasmic tails of TM proteins (106).

Knockdown of talin expression in CHO cells inhibits β1 and β3 integrin activation without altering integrin expression, and this cannot be compensated for by the expression of activating molecules such as activated R-Ras or the CD98 heavy chain (65). Furthermore, talin knockdown blocks agonist-stimulated fibrinogen binding to megakaryocyte integrin αIIbβ3, suggesting that normal cellar activation of integrins also requires talin (65).

Only recently has the structural basis of talin-integrin interaction and its role in integrin activation begun to emerge. THD assumes an extended conformation, instead

of the cloverleaf structure often associated with FERM domains (107). The F3 domain of talin structurally resembles a PTB domain that recognizes ligands containing β turns formed by NPxY motifs (108). In fact, the talin F3 domain binds directly to the integrin β cytoplasmic tails in the MD region containing a conserved NPxY (81,94,109). In addition, the talin F3 domain also interacts with the MP region of the β integrins (80,110). Structural and mutational analyses indicate the importance of both of these interactions in integrin activation. Mutations in talin or integrin that disrupt the talin-integrin association in the MD region (60,61,81,94,109) or in the MP region (80) abolishes talin-dependent integrin activation. Other subdomains of THD enhance activation (111), which may be ascribable to the multiple lipid binding sites found in THD (80,107,112,113). Mutations in these lipid binding sites dramatically decrease talin's ability to activate integrins, supporting the significance of these lipid interactions in integrin activation (80,112,113).

A working model based on the data currently available is that talin binds to the MD region of the integrin β tails, which provides the substantial fraction of the binding energy and facilitates the relatively weaker interaction with the MP region (80,114,115). It is the second interaction that ultimately destabilizes the interaction between the integrin α and β TM and cytoplasmic domains that keeps integrins in an inactivate state (46,56). A Lys residue in the talin F3 domain was recently revealed to form a salt bridge with the conserved Asp residue of the integrin β cytoplasmic tail, and this new salt bridge may potentially disrupt the α-β electrostatic interaction, consequently contributing to the destabilization of the association between the integrin

α and β TM and cytoplasmic domains and thereby to integrin activation (112). In addition, binding of talin to the MD and the MP regions of the β integrins places talin so that the multiple lipid binding sites exposed in the linear arrangement of THD may make an extensive contact with the membrane lipid bilayers (80,107,112,113). This lipid-talin interaction causes a change in the tilt angle of the TM domain of the β integrins, further promoting the separation of the α and the β integrins. Thus, integrin activation can be explained by a series of unique structural events triggered upon talin binding.

RIAM

Talin binding to the integrin β cytoplasmic tails is a final, critical event that must take place for the activation of integrins. Yet, convincing evidence has now accumulated to suggest that 'inside-out' integrin signaling pathway involves more players than simply talin and integrins.

One such molecule is the aforementioned RIAM that has emerged as a key molecule in Rap1-induced, talin-mediated integrin activation (86,92). RIAM binds directly to talin via short, N-terminal sequences predicted to form amphipathic helices as well as to Rap1 through a Ras-association domain (116), therefore acting as a scaffold to bring Rap1 and talin into the 'integrin activation complex' (86). A recent mapping study has generated a minimal Rap1-RIAM module containing a talin-binding site of RIAM fused to the membrane targeting sequences of Rap1, whose expression is sufficient to recruit talin to the membrane and promote talin-dependent

integrin activation (116). RIAM-mediated membrane recruitment of talin was also demonstrated by another study using bimolecular fluorescence complementation assay that showed that RIAM overexpression facilitates and RIAM knockdown blocks talin recruitment to αIIbβ3 integrins in living cells (117). Therefore, one consequence of the formation of the 'integrin activation complex' seems to be RIAM-dependent recruitment of talin to the membrane (86,116,117).

Kindlins

A significant role of kindlin proteins in assisting talin-mediated integrin activation is supported by various recent studies. The mammalian kindlin family of proteins consists of three orthologues, kindlin 1, kindlin 2, and kindlin 3; kindlin 1 and kindlin 2 are widely expressed whereas kindlin 3 is restricted to haematopoietic and endothelial cells (118,119). Kindlins contain a PH domain and a FERM domain (120) and have been shown to bind to β1 and β3 integrins (120,121). Although the F3 domain of kindlins is highly similar to the talin F3 domain (120), the kindlin binding site within the integrin β cytoplasmic tail is the MD NPxY motif, which is distinct from that of talin (122-124).

Mutations in or depletion of kindlin 1 is associated with impaired β1 integrin function and results in defective attachment of epithelial cells to ECM (120,125). Kindlin 2 knockdown in mice also causes defective β1 integrin activation, leading to embryonic lethality similar to β1 integrin null mice (126). Kindlin 3 deficiency in mouse platelets leads to defects in integrin activation and aggregation (122), and loss

of functional kindlin 3 in leukocytes results in impaired β2 integrin activation and leukocyte adhesion (127). In spite of these *in-vivo* data supporting kindlins' role in integrin activation, however, overexpression and knockdown analyses using cell lines present a perplexing picture. For instance, kindlin 3 overexpression activates integrins in a mouse macrophage cell line but does not in CHO cells (122). Although incapable of inducing integrin activation on their own, Kindlin 1 and 2 synergize with THD to activate αIIbβ3 integrins (124). In contrast, they antagonize THD-induced activation of α5β1 integrins (124).

Thus, while there is substantial evidence in favor of an important role for kindlins in the regulation of integrin activation, they may function in a cell type-specific or isoform-specific manner. Moreover, many questions, including those regarding the extent or generality of their involvement and the mechanism of their actions, remain to be answered by future investigation.

Regulation of Talin

Talin binding to the integrin cytoplasmic domains is a key proximal step in integrin activation. It is then critical that we understand how talin and its activities as well as the talin-integrin interaction are regulated. Since integrin activation is tightly controlled as previously discussed, it follows that the talin-integrin interactions are also subject to tight regulation. Yet, despite intense interests and vigorous efforts, we still lack a comprehensive picture of regulatory mechanism governing talin functions.

It has been long speculated that talin is auto-inhibited (86,111,128,129). For example, full-length (FL) talin remains in the cytosol of platelets until the platelets are activated by thrombin, which leads to talin redistribution to the plasma membrane (130) and to the activation of αIIbβ3 integrins. Isolated THD that contains the integrin-binding F3 domain binds to the β3 cytoplasmic tails with sixfold higher affinity than FL talin (129). Accordingly, overexpression of THD is sufficient for strong integrin activation (95) whereas overexpression of FL talin induces modest activation of integrins (86). These earlier observations imply that functions of intact, FL talin may be somehow masked. Indeed, intramolecular, auto-inhibitory interactions are known to regulate activities of other FERM domain-containing proteins (106,129,131,132), favoring a similar regulatory mechanism for talin. The recent *in-vitro* analyses have identified inter-domain interaction between THD and a fragment of the talin rod domain (133,134). It is important to test the biological significance of these findings in the context of talin-mediated integrin activation.

Proteolytic cleavage of intact talin is hypothesized to relieve auto-inhibition of talin by releasing THD which has higher binding affinity for the β tails than FL talin (129,135). In fact, activation of platelets leads to calpain-mediated talin cleavage and αIIbβ3 activation (50). However, as calpain also cleaves the integrin β tails, resulting in activation blockade, the effects of calpain on integrin activation may be more complex (50). Alternatively, binding of PIP2 to talin has also been proposed to induce a conformational change, enhancing the association of talin with the integrin β1 tails (128). Talin can bind to and activate a splice variant of the PIP2-producing enzyme

PIPKIγ-90, stimulating PIP2 production, which in turn could promote the talin-integrin interactions (50). However, as PIPKIγ-90 and integrin binding sites within the F3 domain of talin overlap, PIPKIγ-90 could potentially inhibit talin-mediated integrin activation by interfering the talin-integrin interaction, again complicating the role of PIP2/ PIPKIγ-90 involvement in the regulation of talin during integrin activation.

Another possible mechanism regulating talin binding to the integrin β tails may be the Tyr phosphorylation of the β tail NPxY motif. Phosphorylation of the integrin cytoplasmic domains, such as that mediated by Src family kinases, inhibits talin binding (136), inhibits cell adhesion (137), and displaces integrins from talin-rich sites (138). Tyr phosphorylation of integrins therefore may be an important, negative regulator of integrin activation. However, as Tyr phosphorylation of the β3 integrins occurs after αIIbβ3 integrin activation in platelets, it is not clear whether or not such phosphorylation is important in regulating initial integrin activation (139).

There are many other PTB domain containing proteins that bind to the integrin β tails in a similar fashion to talin (81,109). Such proteins include Numb, DOK-1 and kindlins (81,120). However, talin is unusual in its ability to activate integrins, owing to some unique features only identified in the talin-integrin interaction (80). One such feature, which is absent in other PTB-domain-containing proteins, is the flexible loop between β strands 1 and 2 of the F3 domain of talin (80) that allows interaction with the MP region of the integrin β tail, one of the critical events leading to integrin activation as discussed earlier. In addition, as noted above, THD assumes an unusual

extended conformation (107), and this linear arrangement is expected to align the lipid binding sites along the membrane when the talin F3 domain binds the integrin β tails, further stabilizing the talin-integrin association and favoring activation of integrins (80,107,112,113). Therefore, whereas other PTB-domain-containing proteins may fail to activate integrins due to the lack of these characteristics that are unique to talin, they might antagonize talin during integrin activation by competing for the integrin β tails.

In summary, various mechanisms have been proposed to regulate talin. However, the relative contribution of each of these mechanisms in physiological integrin activation has yet to be defined. Since talin is the central figure that plays a decisive role in integrin 'inside-out' signaling, it is imperative that we gain further understanding of how its functions are regulated.

The text of Chapter 1, in part, is being prepared for publication. Asoka Banno, Benjamin T. Goult, Feng Ye, David R. Critchley, Mark H. Ginsberg. "Functional Mapping of Auto-Inhibitory Sites in Talin". I was the primary investigator of this research as well as the primary author of the manuscript.

Chapter 2:

Methods

Antibodies and cDNAs

Anti- HA mouse monoclonal antibody (MMS101P) was purchased from Covance Research Products Inc. (Denver, PA). Anti-HA rabbit polyclonal antibody (Y-11), anti-Myc mouse monoclonal antibody (9E10), anti-RhoGDI rabbit polyclonal antibody, and anti-His rabbit polyclonal antibody (G18) were from Santa Cruz Biotechnology, Inc. (Santa Cruz, CA). Anti-GFP (Living Colors® Full-Length) rabbit polyclonal antibody was obtained from Clontech (Mountain View, CA). The activation-specific mouse monoclonal PAC1 antibody and αIIbβ3-activating mouse monoclonal anti-LIBS6 antibody were previous described (15,54,141). αIIbβ3-specific competitive inhibitor eptifibatide was obtained from Cor Therapeutics Inc. (South San Francisco, CA) (142,143). R-phycoerythrin-conjugated goat anti-mouse IgM antibody was purchased from Biomeda (Foster City, CA). Ab2308 (16) is an HPLC-purified rabbit polyclonal antibody against anti-αIIb integrins (unpublished data). Mouse monoclonal anti-β3 integrin antibody, AP3 (144), and rabbit polyclonal antibody against β3 cytoplasmic tails, ab8275 (145), have been described previously. Anti-talin mouse monoclonal antibody, 8D4, was obtained from Sigma-Aldrich (St. Louis, MO). Anti-calnexin rabbit polyclonal antibody and anti-LAMP1 (LY1C6) mouse monoclonal antibody were purchased from Abcam. (Cambridge, MA). Anti-lamin A/C rabbit polyclonal antibody was obtained from Cell Signaling Technology

(Danvers, MA). HRP-conjugated anti-mouse IgM antibody was from Jackson ImmunoResearch Laboratories, Inc. (West Grove, PA).

HA-tagged mouse FL wild type (WT) talin and the talin F23 domain (aa 206-405) in mammalian expression vector, pcDNA3.1, have been previously described (86). HA-tagged mouse THD (aa 1-433) was amplified by PCR and subcloned into the mammalian expression pcDNA3-HA vector. Myc-tagged THD was made by PCR using a 5'-primer designed to introduce an N-terminal Myc tag during expression in mammalian cells and subcloning into pcDNA3.1 vector. Point mutations in THD(R358,W359A) mutant were introduced using QuikChangeII XL site-directed mutagenesis kit from Stratagene (La Jolla, CA) with HA-tagged THD as a template and with mutagenic primers. cDNAs encoding mouse talin1 truncation mutants 465 (Tln1(1-465) (aa1-465), Tln1(1-655) (aa1-655), Tln1(1-1654) (aa1-1654), Tln1(1-1822) (aa1-1822), Tln1(1-2298) (aa1-2298), and Tln1(206-450) (aa206-450) were amplified by PCR and subcloned into pcDNA3.1 vector. Each truncation mutant carries a stop codon immediately after the indicated residue number; *e.g.* tln-465 has a stop codon at aa 466. Residue numbers correspond to those of NP_035732.2. The 5'-primer was designed to introduce an N-terminal HA tag during expression in mammalian cells. Deletion of aa1655-1822 (Domain E) was introduced by PCR using a fragment of FL WT flanked by PmlI restriction enzyme sites as a template. When the deletion was confirmed, the PmlI fragment carrying the Domain E deletion was ligated back into the PmlI site of FL WT to produce FL ΔE. Point mutations in FL 5K and FL M319A were introduced using QuikChangeII XL site-directed mutagenesis kit

from Stratagene with FL WT as a template and with mutagenic primers. Deletion of aa434-912 was introduced by PCR using a fragment of FL WT flanked by SnaBI and XhoI restriction enzyme sites as a template. When the deletion was confirmed, the SnaBI-XhoI fragment carrying the deletion was ligated back into FL 5K to produce FL 5K Δ434-912. THD+1823-2541 was created by ligating the PCR-amplified aa1823-2541 fragment to the 3' end of THD using XhoI restriction enzyme site.

RIAM176-CAAX, a talin-binding fragment of RIAM (aa1-176) fused to a Rap1 membrane targeting site, was described previously (116). cDNA encoding GFP-434-450 was generated by PCR amplification from a FL WT cDNA and subcloning into the mammalian expression vector pEGFP-C1. cDNAs encoding GFP-470-486 and GFP-scramble (Scr: GFP-LVNVHGKYVEGASPQRQ) were created by annealing oligos synthesized by Integrated DNA Technologies (San Diego, CA) and subcloning into the pEGFP-C1 vector.

Cell Culture

All the experiments in this study were carried out using CHO cells stably expressing αIIbβ3 integrins (A5 cells) (15), unless noted otherwise. A5 cells were cultured in Dulbecco's modified Eagle's medium supplemented with non-essential amino acids, *L*-glutamine, antibiotics, and 10% fetal calf serum.

Subcellular Fractionation

A5 cells, transiently transfected with indicated cDNAs for 24 hours, were subjected to subcellular fractionation as described before (86). In brief, cells were harvested in fractionation buffer (20mM HEPES-KOH pH7.5, 1.5mM $MgCl_2$, 5mM KCl, 0.2mM Na_3VO_4, 10ug/mL leupeptin, 10ug/mL aprotinin, 1mM PMSF, and Complete mini protease inhibitor tablet (Roche Applied Bioscience, Indianapolis, IN)) and incubated on ice for 10 min. Swollen cells were disrupted by shearing method through 27G needles, and a fraction of the total cell lysate was saved for analysis of total protein expression. The remaining lysates were centrifuged at 2000 rpm for 10 min to pellet nuclei and unbroken cells. The supernatant was further centrifuged at 14,000 rpm for 30 min to pellet the membrane fraction. Membrane-containing pellet was washed and then incubated in the fractionation buffer containing 1% Nonidet P-40 on ice. Samples were run on SDS-PAGE gels (Invitrogen, Carlsbad, CA), and expression of talin in total lysates, cytosolic, and membrane fractions were analyzed by Western blotting using anti-HA antibody. Integrin αIIb-specific Rb2308 and anti-RhoGDI antibodies were used as membrane and cytsolic markers, respectively. The bands corresponding to the membrane and cytosolic fractions were scanned and quantified with Odyssey infrared imaging system from Li-Cor Biosciences (Lincoln, NE), and represented as percent of total (cytosolic + membrane).

In-Vivo Integrin Activation Assay

PAC1 binding assessing αIIbβ3 integrin activation was measured by three-color flow cytometry as previously described (54). Briefly, after A5cells were transiently co-transfected with HA-tagged talin and GFP-only or GFP-tagged RIAM176-CAAX for 24 hours, they were suspended and stained first with PAC1 alone (140), in the presence of αIIbβ3-specific competitive inhibitor eptifibatide (141,142), or in the presence of αIIbβ3-activating anti-LIBS6 antibody (15,54), and then with R-phycoerythrin-conjugated goat anti-mouse IgM antibody on ice. PAC1 binding to live (propidium iodide-negative), transfected (GFP-positive) cells were then measured with a FACScan instrument (Becton Dickinson, Mountain View, CA). The collected data were analyzed with Cellquest software (Becton Dickinson). To obtain numerical estimates of integrin activation, we calculated an activation index, defined as $100 \times (F - F_0) / (F_{max} - F_0)$, where F is the median fluorescence intensity (MFI) of PAC1 binding alone, F_0 is the MFI of PAC1 binding in the presence of eptifibatide, and F_{max} is the MFI of PAC1 binding in the presence of anti-LIBS6 antibody. Data are then presented as percent increase over empty pcDNA vector-transfected cells.

In talin trans inhibition experiment, THD was co-transfected with GFP-434-450, GFP-Scr, GFP-470-486, or GFP.

Purification of Plasma Membrane-Associated Proteins

After 24 hour transient-transfection with indicated cDNAs, A5 cells were detached with 5mM EDTA/PBS and subjected to surface biotinylation with 3mM EZ-

Link Sulfo-NHS-Biotin (Thermo Fisher Scientific, Rockford, IL) dissolved in 0.1M sodium phosphate buffer, pH8.0, for 30 min. Cells were then washed extensively with PBS and subjected to subcellular fractionation described above. Pelleted crude membranes were then resuspended in fractionation buffer and incubated with BcMag™ Streptavidin Magnetic Beads (Bioclone Inc, San Diego, CA) for an hour at room temperature with rotation to separate plasma membrane from intracellular organelle membranes. Whole cell, nuclear/Intact cell, cytosolic, and crude membrane fractions were saved for subsequent western blot analysis. Bound proteins were washed and eluted with SDS sample buffer. Samples were run on SDS-PAGE gels, and expression of transfected talin in each fraction was analyzed by western blotting using anti-HA or anti-Myc antibody. Endogenous FL-talin was detected with anti-talin 8D4 antibody. RIAM176-CAAX was detected by anti-GFP antibody. Integrin αIIb-specific Rb2308, anti-calnexin, anti-lamin A/C, anti-LAMP1, and anti-RhoGDI antibodies were used as plasma membrane, ER membrane, nuclear membrane, lysosomal membrane, and cytsolic markers, respectively. The bands corresponding to talin and αIIb integrins in the whole cell lysates and in the plasma membrane fraction were quantified with Odyssey infrared imaging system from Li-Cor Biosciences, and proteins detected in the plasma membrane fraction was calculated as percent of total. Talin observed in the plasma membrane fraction were then normalized by αIIb integrin signal in the same fraction and is represented as percent plasma membrane association.

Co-Immunoprecipitation Assay

Immunoprecipitation assay employed here was modified from the protocol of Humphries, *et al*. (145). After 24 hour transient-transfection, A5cells or CHO-K1 cells that do not express αIIbβ3 integrins were rinsed and trypsinized. $5x10^5$cells from each sample were taken, rinsed, and resuspended to the final concentration of $1x10^6$cells/mL in PBS, supplemented with 2mM EDTA, pH7.4. Each reaction was then incubated with 50 μL anti-β3 antibody (AP3)-coupled magnetic beads for 30 min at 4°C with rotation. AP3 was conjugated to tosylactivated paramagnetic Dynabeads M-450 (Invitrogen) as instructed by the manufacturer's protocol. Bead-bound cells were isolated on a magnet and washed with CSK buffer (10mM PIPES pH6.8, 50mM NaCl, 150mM sucrose, 3mM MgCl2, 1mM MnCl2, pH6.8) supplemented with 20mM Tris-HCl, pH8.0, and 2mM Na_3VO_4. After the last wash, cells were lysed with CSK lysis buffer (CSK buffer, 0.5% (v/v) Triton X-100, 2mM Na_3VO_4, Complete mini protease inhibitor tablet (Roche Applied Bioscience) for 10min with rotation. After cell lysis, samples were washed with CSK lysis buffer, and affinity-purified proteins were eluted from the magnetic beads with SDS sample buffer. Proteins were separated on SDS-PAGE gels (Invitrogen). Bound talin was detected by western blotting using anti-HA rabbit polyclonal antibody, and the bands were scanned and quantified with Odyssey infrared imaging system from Li-Cor Biosciences. β3 integrin capture was verified with anti-β3 rabbit polyclonal antibody ab8275. The band intensity for each sample was normalized by the corresponding input to adjust for the possible inequality in starting material. Talin association observed in CHO-K1

cells was subtracted from that in A5 cells for each sample, to give β3-dependent association. THD was then set as the maximal association capacity.

Affinity Chromatography

10ug of purified recombinant His-Avi-β3 cytoplasmic tail coupled to neutravidin agarose resin (Thermo Fisher Scientific) was incubated overnight at 4°C with increasing amounts of purified recombinant His-tagged THD, Tln1(1-465), or Tln1(1-1654) proteins in buffer (10 mM PIPES, 50 mM NaCl, 150mM Sucrose, 1% Triton X-100, 50mM NaF, 40mM $Na_4P_2O_7 \cdot 10H_2O$, 1mM Na_3VO_4, and Complete mini protease inhibitor tablet (Roche Applied Bioscience), pH 6.8). Samples were then separated on SDS-PAGE gels (Invitrogen). Bound talin was detected by western blotting using anti-His antibody, and the bands were scanned and quantified with Odyssey infrared imaging system from Li-Cor Biosciences. THD was then set as the maximal binding capacity. Equal loading of β3 cytoplasmic tails was verified by gel staining with Imperial Protein Stain (Thermo Fisher Scientific).

***In-Vitro* Integrin Nanodisc Assay**

Integrin nanodisc assembly/purification and activation assay were described in Ye, *et al*. (99). Briefly, in nanodiscs, αIIbβ3 integrin purified from outdated human platelets were inserted into two lipid layers composed of DMPC and DMPG and held together by membrane scaffold protein (MSP). The assembled integrin nanodiscs were purified and separated from empty nanodiscs using a HiLoad 16/60 Superdex

200 size exclusion column (GE Healthcare, Piscataway, NJ) with TBS. Their successful assembly was also confirmed by staining of the SDS-PAGE gels with Imperial Protein Stain (Thermo Fisher Scientific).

Integrin nanodiscs were captured onto a micro-titer plates via anti-β3 AP3 antibody by 3-hour room temperature incubation, followed by another 3-hour room temperature incubation with various concentrations of THD, Tln1(1-465), or Tln1(1-1654). Integrin activation was assessed with PAC1 binding followed by HRP-conjugated anti-mouse IgM. After the last wash, signals were detected with ECL reagent and read by a Victor2 luminescence plate reader. PAC1 binding in the presence of eptifibatide served as negative control. Specific binding was then calculated as $L-L_0$, where L = luminescence intensity and L_0 = luminescence in the presence of eptifibatide. For each talin protein, result is represented as percent increase over 0μM point in specific PAC1-binding.

In trans inhibition experiment, 5.0uM of THD was mixed with 0.1uM of GST-434-450, GST-Scr, or GST.

Expression and Purification of Recombinant Talin Proteins

His-tagged THD and Tln1(1-465) in pET28 bacterial expression vector have been previously described (99). For the His-tagged Tln1(1-1654) expression plasmid, PCR fragment containing aa1-1654 of human talin1 was cloned into pET28 bacterial expression vector that attaches a His-tag on the N-terminus (EMD Chemicals, Gibbstown, NJ). Residue numbers are based on NP_006280.3.

Purification protocol for the THD and Tln1(1-465) was described in Ye, *et al*. (99). Tln1(1-1654) recombinant protein was expressed in *Escherichia coli* BL21-DE-pLys and purified with His-binding beads according to the manufacturer's instructions (EMD Chemicals). The purified protein was dialyzed against TBS and then ran through a hi-load 16/60 Superdex 200 size exclusion column with TBS to remove smaller fragments generated by proteolytic cleavages during purification.

The cDNAs encoding mouse talin1 residues 196-405 (F23), 196-309 (F2), 309-400 (F3), 482-655 (vinculin binding site (VBS)1), 655-787 (VBS2a), 787-911 (VBS2b), 482-787 (VBS1/2a) and 482-911 (VBS1-VBS2a-VBS2b) were synthesized by PCR using a mouse talin1 cDNA as template and cloned into the expression vector pET-151TOPO (Invitrogen). These talin polypeptides were expressed in *E.Coli* BL21 STAR (DE3) cultured in either LB for unlabelled protein or in M9 minimal media for preparation of isotopically labelled samples for NMR analysis. Recombinant His-tagged talin polypeptides were purified by nickel-affinity chromatography following standard procedures. The His-tag was removed by cleavage with AcTEV protease (Invitrogen), and the proteins were further purified by anion-exchange or cation-exchange depending on the construct.

GST-434-450 and GST-Scr were generated by digesting the corresponding fragments out of pEGFP-C1 vector with restriction enzymes and inserting them into the bacterial expression vector pGEX. GST-434-450, GST-Scr, and GST recombinant proteins were expressed in *Escherichia coli* BL21-DE-pLys and purified with

GlutathioneSepharose 4 FastFlow agarose according to the manufacturer's instructions (GE Healthcare). The purified proteins were dialyzed against TBS.

Protein concentrations were determined using their respective extinction coefficient at 280 nm. Protein concentrations were based on absorption coefficients calculated from the aromatic content according to ProtParam (www.expasy.org).

NMR Spectroscopy

NMR experiments for the resonance assignment of talin aa482-655, aa655-787, and aa787-911 were carried out with 1mM protein in 20mM sodium phosphate pH 6.5, 50mM NaCl, 2mM DTT, 10% (v/v) $^{2}H_2O$ by my collaborator Benjamin T. Goult (University of Leicester, UK). NMR spectra of all the proteins were obtained at 298K using Bruker AVANCE DRX 600 or AVANCE DRX 800 spectrometers both equipped with CryoProbes (Bruker, Coventry, UK). Proton chemical shifts were referenced to external DSS, and ^{15}N and ^{13}C chemical shifts were referenced indirectly using recommended gyromagnetic ratios (146). Spectra were processed with TopSpin (Bruker) and analyzed using Analysis (147). 3D HNCO, HN(CA)CO, HNCA, HN(CO)CA, HNCACB, and HN(CO)CACB experiments were used for the sequential assignment of the backbone NH, N, CO, Cα, and Cβ resonances. The resonance assignments of aa482-655, aa655-787, and aa787-911 have been deposited in the BioMagResBank (BMRB) (http://www.bmrb.wisc.edu) with the accession numbers 17555, 17350, and 17332, respectively. The NMR assignments of the F2 and F23 domains were deposited in the BMRB database and published previously (148); F2

(aa196-309), BMRB ID = 16930; F3 (aa309-405), BMRB ID = 7150; F23 (aa196-405), BMRB ID = 16932. Resonance assignments were then transferred to the double domain aa482-787 using the single domains assignments and confirmed using a HNCA collected on aa482-787.

NMR Titrations

All titrations were carried out in 20mM phosphate pH6.5, 50mM NaCl, 2mM DTT by my collaborator Benjamin T. Goult (University of Leicester, UK). A series of ^{15}N-HSQC spectra were measured for the ^{15}N-labelled protein alone and then in the presence of increasing amounts of unlabelled fragments of talin. Initially, ^{15}N-labelled F23 was screened against the five large fragments of talin aa1-433, aa434-911, aa913-1653, aa1655-2294, and aa2300-2541.

The text of Chapter 2, in part, is being prepared for publication. Asoka Banno, Benjamin T. Goult, Feng Ye, David R. Critchley, Mark H. Ginsberg. “Functional Mapping of Auto-Inhibitory Sites in Talin”. I was the primary investigator of this research as well as the primary author of the manuscript.

Chapter 3:

Results

Domain E – Bulk Membrane Association

As noted above, THD contains multiple lipid binding sites that could serve in membrane interactions (80,107,112,113), and previous studies raised the possibility that such sites might be masked by the talin rod domain. To test the role of the rod domain in membrane recruitment in cells, we used subcellular fractionation to compare the localization of THD with that of FL WT talin. Approximately 50% of THD was found in the membrane fraction whereas only ~20% of FL WT talin was in this fraction (Fig. 1A), thus confirming that the membrane-targeting sites in THD are masked in FL WT talin. Furthermore, in agreement with previous observations that translocation of talin from the cytosol to the peripheral membrane accompanies platelet activation (130,149), we found that the membrane association of talin coincided with its capacity to increase αIIbβ3 integrin affinity for ligands; THD consistently induced a fourfold greater increase in activation compared with FL WT talin (Fig. 1B). Expression of the talin binding fragment of RIAM fused to a Rap1A membrane targeting site (RIAM176-CAAX), which promotes association and interaction of talin with integrins (116), led to increased membrane recruitment of FL WT talin and integrin activation (Fig. 1A and B). Thus, the presence of the talin rod domain inhibits the capacity of THD both to associate with the membrane and to induce integrin activation.

These results supported the idea that the rod domain might contain auto-inhibitory regions. To localize the inhibitory site(s), we constructed a series of C-terminal truncations of talin and examined the localization of these mutants by subcellular fractionation. The rod domain of talin comprises 62 amphipathic α-helices that are assembled into a series of α-helical bundles (150,151). Therefore, to avoid disrupting the tertiary structure of the resulting protein, we introduced each stop codon in between α-helical bundles as designated by arrowheads in Figure 2A. Talin1 1-1654 (Tln1(1-1654)) showed markedly increased membrane association, approaching that of THD (Fig. 2B ; 43± 1.5 and 58 ± 7.6%, respectively). In contrast, Tln1(1-1822) and Tln1(1-2298) showed membrane association that was similar to that observed for FL WT talin (Fig. 2B; 18 ± 2.0, 5.7 ± 2.1, and 9.1 ± 3.2%, respectively). The membrane marker, αIIb integrin, and the cytosolic marker, RhoGDI, were detected only in the membrane and the cytosolic fractions, respectively, validating the subcellular fractionation. These data suggest that the loss of the five helix bundle contained within talin aa1655-1822, termed Domain E (134), increases membrane recruitment of talin. To test the effect of loss of Domain E, we deleted it in the context of the FL talin protein (FL ΔE) (Fig. 3A). FL ΔE also exhibited markedly increased membrane association (Fig. 3B; 41 ± 4.6%). Thus, Domain E inhibits membrane recruitment of talin.

Previous studies used NMR to demonstrate that the talin rod domain interacts with the F3 domain of talin FERM domain (133,134). One of these NMR analyses indicated five acidic residues in Domain E (Fig. 4A; Asp1676, Asp1763, Glu1770,

Glu1798, and Glu1805, shown in red) that form an interface with a basic surface in the F3 domain (134). Reverse-charge mutations were made at each of the five residues (FL 5K), which lie at the interface, to disrupt the electrostatic association between Domain E and the F3 domain. Basic residues on the F3 domain that are in contact with the above-mentioned Domain E acidic residues are colored in blue (Fig. 4A; Lys316, Lys318, Lys320, Lys322, Lys324, and Lys364). FL 5K showed increased membrane association (Fig. 4B; 44 ± 6.0%), similar to that seen with Tln1(1-1654) and FL ΔE (Fig. 2B and 3B, respectively). Therefore, the DomainE-F3 interaction blocks talin membrane recruitment.

Goksoy, *et al.* reported that the THD-talin rod interaction can be disrupted by a single M319A point mutation in the F3 domain (133). However, the residue Met319, colored in black in Figure 4A, appears not to be in the interface between Domain E and the talin F3. Assessment of FL M319A localization showed that, in contrast to FL ΔE and FL 5K mutants (Fig. 3B and 4B, respectively), FL M319A membrane localization was similar to that of FL WT (Fig. 4C; 11 ± 1.7 and 13 ± 4.0%, respectively). Thus, specific interactions between Domain E and THD restrict membrane recruitment of talin.

Earlier work (86,116,117,130,149) and the present study (Fig. 1A and B) show that membrane localization of talin correlates with its ability to activate integrins. To test whether increased membrane association of talin by truncation (Tln1(1-1654)), Domain E deletion (FL ΔE), or Domain E point mutations (FL 5K) leads to integrin activation, we monitored integrin activation induced by these talin mutants in cells

expressing recombinant αIIbβ3 integrins. αIIbβ3 integrin activation was measured by flow cytometry, using PAC1, an activation-specific αIIbβ3 antibody (140). Tln1(1-1654), FL ΔE, and FL 5K were similar to FL WT talin, inducing minimal increases in PAC1 binding, whereas THD induced a dramatic increase (Fig. 5). As it may be expected based on its little association with the membrane fraction (Fig. 4C), FL M319A induced only small increase in PAC1 binding (Fig. 5). Thus, the loss of Domain E and the disruption of the Domain E-F3 interaction, which markedly increase the efficiency of membrane recruitment of talin to levels similar to that seen with THD, failed to have a proportional effect on integrin activation. Hence, membrane recruitment of talin is insufficient for talin-mediated integrin activation.

To verify that these mutants are indeed capable of activating integrins, we used a previously described method of enforcing the talin-integrin interaction with RIAM176-CAAX (116). Co-expression of RIAM176-CAAX increased integrin activation in cells expressing each of the talin mutants (black bars in Fig. 5), indicating that the talin mutants retained the capacity to activate integrins if they associate with and interact with integrins. Thus, mutations that led to localization of talin to the membrane fraction are not sufficient to enable talin to activate integrins efficiently, suggesting that additional auto-inhibitory sequences in talin lie between residues 434 (the C terminus of THD) and 1654.

Integrin-activating signals cause talin to translocate from the cytosol to the plasma membrane (130,149). Our subcellular fractionation assay, however, did not distinguish the cell surface plasma membrane from membranes of intracellular

organelles. To test whether the failure of Tln1(1-1654) to activate integrins might be due to its inability to localize to the plasma membrane, we slightly modified our fractionation protocol to separate the plasma membrane from intracellular membranes. Cells expressing THD and Tln1(1-1654) were labeled with cell-impermeable sulfo-biotin. After disruption and subsequent fractionation steps, the plasma membrane was further purified by capture with streptavidin-conjugated magnetic beads, and the association of talin with the recovered plasma membrane was examined. Although initial subcellular fractionation showed similar levels of Tln1(1-1654) and THD in the crude membrane fraction (Fig. 2B), the abundance of Tln1(1-1654) was markedly reduced in the purified plasma membrane fraction relative to that of THD (Fig. 6; 18 ± 5.5 and 65 ± 7.5%, respectively). As expected, FL WT talin was almost undetectable in this fraction (Fig. 6). Presence of αIIb integrin (plasma membrane marker) and the absence of calnexin (ER membrane marker), lamin A/C (nuclear membrane marker), LAMP1 (lysosomal membrane marker), and RhoGDI (cytosolic marker) confirmed the enrichment of the plasma membrane (Fig. 6). Thus, although the loss of Domain E increases the association of talin with bulk membranes, it fails to target talin specifically to the plasma membrane.

In addition to plasma membrane localization, talin binding to the integrin β cytoplasmic tails is an essential event leading to integrin activation (65,95-98). To determine whether Tln1(1-1654) is also defective in this function, we immunoprecipitated the β3 integrins from cells expressing THD, Tln1(1-1654), or FL WT and compared the interaction between αIIbβ3 integrins and these talin variants.

Compared to THD, Tln1(1-1654) showed reduced association with αIIbβ3 integrins similar to that exhibited by FL WT (Fig. 7A). To confirm that the reduced association of talin with αIIbβ3 was due to reduced binding to the β3 cytoplasmic domains, we performed affinity chromatography with the purified recombinant β3 integrin tail model proteins (152,153). Both Tln1(1-1654) and FL WT bound to the β3 integrin cytoplasmic tails to a lesser degree than THD (Fig. 7B). Nonspecific binding to the purified recombinant αIIb cytoplasmic tails was comparable between three proteins, confirming the specificity of the talin-β3 integrin interactions observed in the experiment (Fig. 7B). These data together with results from preceding experiments suggest that, although Tln1(1-1654) shows increased association with the crude membrane fraction, it is impaired in its ability both to localize to the plasma membrane and to efficiently interact with the β3 cytoplasmic tails.

We then asked whether the β3 integrin binding of talin is required for its plasma membrane localization, *i.e.* if the ability to interact with integrins is necessary for plasma membrane localization of talin. To address this question, we isolated the plasma membrane fraction from cells expressing THD(R358,W359A), a previously-characterized mutant with dramatically reduced integrin binding (109). THD(R358,W359A) was present in the plasma membrane fraction at similar abundance to THD (Fig. 8; 81 ± 37 and 54 ± 10%, respectively), indicating that plasma membrane localization of talin does not require β3 integrin binding.

Next, we used a recently established *in-vitro* integrin nanodisc assay (99) to determine whether plasma membrane localization assures that talin interacts with the

β3 integrin cytoplasmic tails. This assay is composed of αIIbβ3 integrins purified from human platelets, inserted into nanodiscs comprising a lipid bilayer encircled by a membrane scaffold protein (MSP), and purified recombinant talin or talin fragments (99). αIIbβ3 integrin activation was measured by PAC1 binding. At every protein concentration of talin tested, Tln1(1-1654) was less active than THD in inducing integrin activation (Fig. 9), which is consistent with the data from cell-based integrin activation assay (Fig. 5). One of the important features of this nanodisc system is to recreate the final event in integrin activation, the talin-integrin interaction at the plasma membrane; the results also indicate that Tln1(1-1654) is impaired in its ability to associate with αIIbβ3 integrins and are in agreement with the observations from co-immunoprecipitation assay (Fig. 7A) and from affinity chromatography (Fig. 7B). Moreover, the nanodisc data suggest that plasma membrane localization may not necessarily enable talin to interact with the integrin cytoplasmic tails. Thus, talin sequences between aa434 and aa1654 inhibit talin's ability to target to the plasma membrane and to bind to the β3 integrin cytoplasmic tails.

VBS1/2a – Plasma Membrane Localization

The foregoing data indicate that plasma membrane localization and integrin binding of Tln1(1-1654) are limited by sequences between aa434 and aa1654. To determine if this region of the rod domain limits talin's functions by making another inter-domain interaction with a region in THD, my collaborator Benjamin T. Goult at University of Leicester, UK, performed NMR spectroscopy using ^{15}N-labelled talin

F23 domain with various fragments of the talin rod domain (Table 1). He found that the F23 domain of talin interacted with another helical bundle called VBS1/2a (154) (Fig. 10A and Table 1). Likewise, ^{15}N-HSQC spectra of ^{15}N-labelled VBS1/2a in the presence of different fragments of talin confirmed its interaction with THD (Fig. 10A and Table 1). To further characterize these interactions, he assigned the backbone chemical shifts of VBS1, VBS2a, and VBS2b. This enabled the application of chemical shift mapping to identify the peaks that are affected and to map them onto the surface of the known structures of the protein domains involved. Interestingly, observed shifts in signals and broadening effects were mapped predominantly over one face of each fragment (Fig. 10B), implying a specific interaction between those surfaces of the two domains. Furthermore, this inter-domain interaction with the F23 domain appears to require both VBS1 and VBS2a as a single module, as analysis of VBS1 or VBS2a separately with the F23 domain did not result in significant chemical shift changes (data not shown).

To determine whether VBS1/2a is involved in the regulation of talin plasma membrane localization, we created two more truncation mutants (Fig. 2A), Tln1(1-465) and Tln1(1-655), and examined their association with the plasma membrane fraction. The abundance of Tln1(1-655) was similar to that of Tln1(1-1654) and FL WT (Fig. 11; 30 ± 3.4, 23 ± 2.8, and 22 ± 2.0%, respectively). In contrast, Tln1(1-465) exhibited markedly increased association with the plasma membrane fraction equivalent to that of THD (Fig. 11; 67 ± 8.8 and 54 ± 12%, respectively). These data

indicate that the loss of VBS1/2a leads to plasma membrane localization and suggests that VBS1/2a is the inhibitor of this particular function of talin.

The aa434-450 Linker Fragment – Interaction with Integrin β Cytoplasmic Tails

We then asked if truncation of VBS1/2a module (Tln1(1-465)) potentiates talin-induced integrin activation. αIIbβ3 integrin activation in cells expressing THD, Tln1(1-465), Tln1(1-1654), and FL WT was measured by flow cytometry using PAC1 antibody. All the talin mutants tested, except for THD, showed minimal increases in PAC1 binding (Fig. 12A), indicating that the loss of VBS1/2a was not sufficient to induce talin-mediated integrin activation and implying that another talin sequence, namely the fragment contained within the residues 434 and 465, still restricts talin's activity. This fragment lies within the linker region found between THD and the rod domain (Fig. 2A) and is known to be largely unstructured. This third inhibitory site was further narrowed down to the 17-residue fragment between aa434 and aa450 (data not shown).

In addition to THD, the isolated talin F23 domain also represents an active fragment of talin capable of stimulating integrin activation, albeit slightly more weakly than THD (86,111). If the aa434-450 fragment indeed blocks talin-dependent integrin activation, we hypothesized that attachment of this fragment to the C terminus of the F23 domain (Fig. 12B; Tln1(206-450)) could suppress integrin activation induced by this otherwise activating fragment of talin. Comparison of PAC1 binding indicated that F23-mediated integrin activation was reduced by approximately 60% in

cells expressing Tln1(206-450), supporting the inhibitory effect of the aa434-450 fragment (Fig. 12B).

Next, we investigated whether the isolated aa434-450 fragment could have a *trans* inhibitory effect on THD. We made a GFP-tagged aa434-450 fragment (GFP-434-450) as well as two negative controls, one being a scrambled sequence of the aa434-450 (GFP-Scr; GFP- LVNVHGKYVEGASPQRQ) and the other a fragment of the same length taken farther C-terminal of talin (GFP-470-486). αIIbβ3 integrin activation was then assessed in cells co-expressing THD and either one of these GFP-tagged fragments. Compared to GFP-only, GFP-434-450 strongly suppressed THD-mediated integrin activation without affecting the expression of THD (Fig. 13A; 60 ± 7.7% inhibition), whereas the effects of GFP-Scr and GFP-470-486 were much smaller (Fig. 13A and B; 17 ± 11 and 15 ± 7.9% inhibition, respectively). Therefore, the aa434-450 fragment of talin specifically suppresses talin-mediated integrin activation and could do so in a *trans* manner.

Truncation of VBS1/2a releases the inhibition on plasma membrane localization of talin (Fig. 11), leading us to hypothesize that the aa434-450 fragment may interfere with the talin-integrin interaction. To test this idea, we performed *in-vitro* affinity chromatography to compare binding of the purified recombinant THD and Tln1(1-465) to the purified recombinant β3 cytoplasmic tails. The data indicated that Tln1(1-465) bound less efficiently to the β3 cytoplasmic tails than THD did at every protein concentration examined (Fig. 14; *e.g.* 81 ± 3.4% of the maximal THD binding at 200nM).

The integrin tail binding data were substantiated by the results from the aforementioned integrin nanodisc assay comparing PAC1 binding induced by THD and Tln1(1-465). Tln1(1-465) was much less potent in activating integrins than THD in this *in-vitro* system (Fig. 15A; *e.g.* 46.8 ± 11.4 and 152 ± 21.2% increase at 25uM, respectively). As noted earlier, integrin nanodisc system allows us to study the talin-integrin interaction required for integrin activation in a more controlled environment than cell-based assays. With αIIbβ3 integrins inserted into the plasma membrane-like phosphoslipid nanodiscs, it also provides a more physiologically-relevant context for the analysis of the talin-integrin association than conventional *in-vitro* affinity chromatography. Thus, the data here strongly support the inhibitory effect of the aa434-450 fragment on talin binding to the integrin β cytoplasmic tails and integrin activation.

The aa434-450 fragment of talin was able to specifically suppress talin-mediated integrin activation in a *trans* manner in cells (Fig. 13A and B). Therefore, to examine whether the aa434-450 fragment exhibits the same *trans* inhibitory effect in the *in-vitro* integrin nanodisc system, we measured THD-induced PAC1 binding to integrin nanodiscs in the presence of GST-434-450 or GST-Scr. Measurements of PAC1 binding indicated that GST-434-450 strongly and specifically suppressed THD-mediated integrin activation in this purified system, compared to the GST-Scr control (Fig. 15B; 86 ± 17 and 28 ± 4.1% inhibition, respectively). Together, these data demonstrate that the talin aa434-450 fragment specifically hinders the talin-β3 cytoplasmic tail interaction, thereby inhibiting talin-mediated integrin activation.

Steric Hindrance

We have so far identified three distinct sites within talin that inhibit specific activities of talin. Domain E and its interaction with the talin F3 domain prevent association of talin with membranes, thereby keeping FL talin in the cytosol. VBS1/2a restricts localization of talin to the plasma membrane. The aa434-450 fragment found within the flexible linker region of talin between THD and the rod domain interferes with the talin-β3 cytoplasmic tail interaction. Now, we hypothesized that deletion of all three sites may lead to a constitutively active form of FL talin that can induce integrin activation as efficiently as THD does. To test this idea, we constructed a talin mutant, FL5K Δ434-912, in which deletion of the aa434-450 fragment and VBS1/2a was combined with 5K mutations in Domain E that disrupt the DomainE-F3 interaction. αIIbβ3 integrin activation induced by FL5K Δ434-912 was however no different from FL WT (Fig. 16A). Expression levels were comparable amongst the talin proteins. Furthermore, co-expression of RIAM176-CAAX increased integrin activation in cells expressing FL5K Δ434-912 as well as FL WT (data not shown), indicating that the mutation did not affect the capacity of resulting protein to activate integrins when forced to associate with and interact with integrins. Thus, concomitant deletion of the three inhibitory sites is insufficient for talin-mediated integrin activation.

Integrin activation requires two integrin binding sites located within the F3 domain (80,81,94,109,110) and three lipid association regions found in the F1, F2, and F3 domains of talin (80,107,112,113). These multiple interactions may be optimized

only when THD is oriented precisely and perfectly with respect to integrins and the plasma membrane. Moreover, this particular positioning of THD can possibly be obstructed by any bulky module in a non-specific, steric fashion. We therefore reasoned that the ability of THD to interact with integrins might still be hindered by the presence of the remaining rod domain in the mutant FL5K Δ434-912, even in the absence of the inhibitory sites. To test this hypothesis, we attached a fragment of the talin rod domain C-terminal of Domain E to THD (THD+1823-2541) and examined the effect of this rod fragment on THD-mediated integrin activation. The aa1823-2541 fragment was chosen because truncation of this region had no effect on membrane localization of talin or integrin activation (Fig. 2B and 5). αIIbβ3 integrin activation by THD was reduced by the attachment of the aa1823-2541 fragment in THD+1823-2541 mutant (Fig. 16B). Again, co-expression of RIAM176-CAAX increased integrin activation by this mutant (data not shown), assuring the functionality of the protein. Thus, presence of a large module can non-specifically and sterically prevent talin from activating integrins.

The text of Chapter 3, in part, is being prepared for publication. Asoka Banno, Benjamin T. Goult, Feng Ye, David R. Critchley, Mark H. Ginsberg. "Functional Mapping of Auto-Inhibitory Sites in Talin". I was the primary investigator of this research as well as the primary author of the manuscript.

Figure 1

Functions of talin are negatively regulated by the rod domain.

A. After 24 hour transfection, A5 cells expressing THD, FL WT, or FL WT with RIAM176-CAAX were subjected to subcellular fractionation, and talin distribution was assessed by western blotting with anti-HA antibody. Integrin αIIb and RhoGDI were used as markers for the membrane and cytsolic fractions, respectively. The blots were quantified by densitometric scanning, and each fraction was calculated and is represented here as percent of total (cytosolic + membrane). Results represent mean ± standard error (SE) ($n \geq 3$). A representative blot is shown (C, M, and WCL indicate cytosolic fraction, membrane fraction, and whole cell lysates, respectively). B. A5 cells were transfected with cDNAs encoding THD or FL WT along with GFP or GFP-tagged RIAM176-CAAX, as indicated. Twenty-four hours later, αIIbβ3 integrin activation was examined by flow cytometry using the activation-specific antibody, PAC1. The activation indices were calculated as described in "Methods" and are presented as percent increase over basal activation observed with empty pcDNA vector-transfected cells. Results represent mean ± SE ($n \geq 3$). Expression levels of transfected proteins were verified by western blotting.

Figure 1

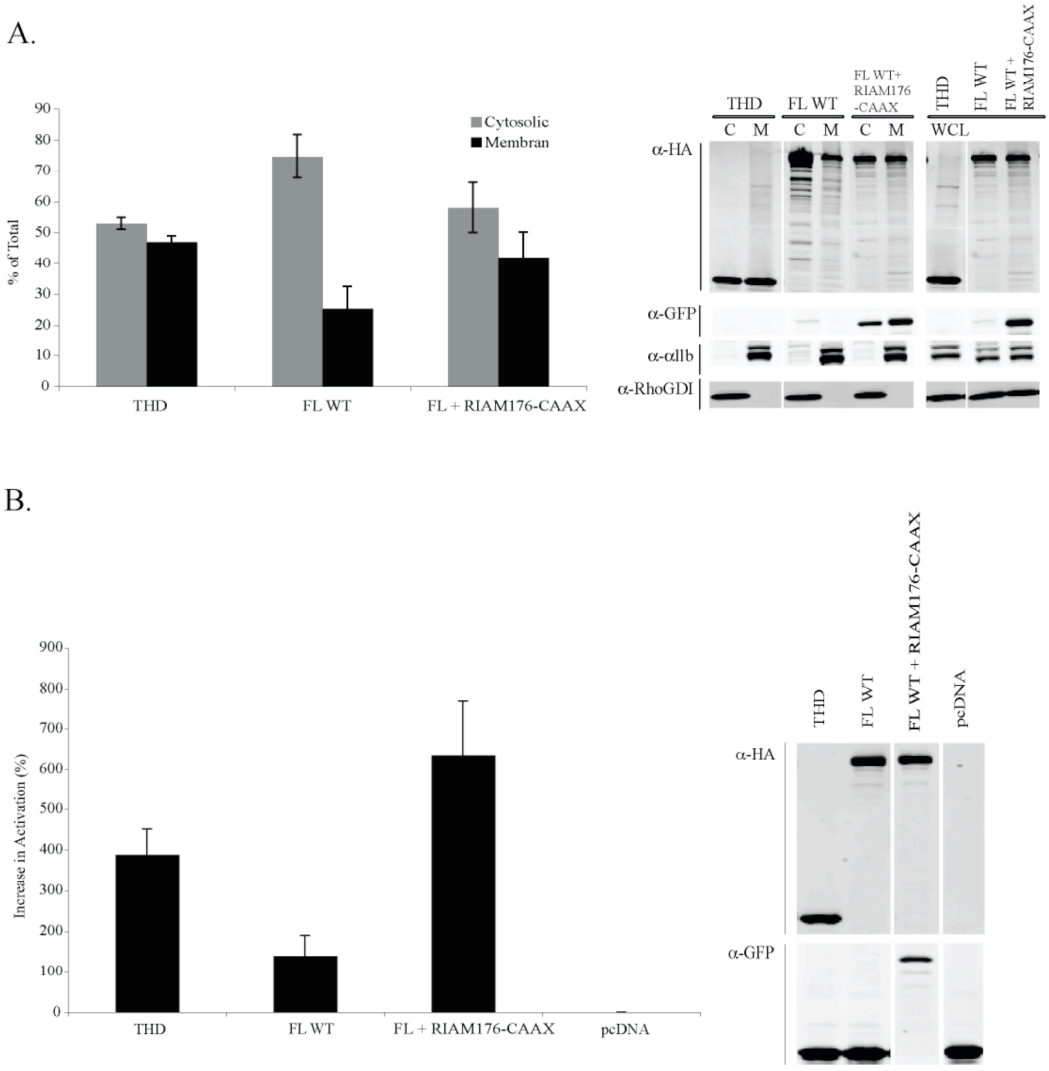
A.
% of Total
Cytosolic
Membran
THD
FL WT
FL + RIAM176-CAAX
FL WT+ RIAM176 -CAAX
C M
WCL
α-HA
α-GFP
α-αIIb
α-RhoGDI
B.
Increase in Activation (%)
pcDNA
FL WT + RIAM176-CAAX

Figure 2

Truncation of Domain E results in increased association of talin with membranes. A. Schematic diagram of talin: talin consists of THD (aa1-433) and a rod domain (aa482-2541) connected by a linker region. THD contains an F0 domain and a FERM domain that can be sub-divided into the F1, F2, and F3 domains. The rod domain is a series of α-helical bundles, one of which is Domain E located between aa1655 and aa1822. VBS1 and VBS2a corresponding to aa 482-655 and aa 656-787, respectively, are also shown. Arrowheads indicate the truncations made in this study. B. A5 cells transfected with the indicated talin constructs were subjected to subcellular fractionation, and distribution of talin was assessed by western blotting with anti-HA antibody. Integrin αIIb and RhoGDI served as the membrane and cytsolic markers, respectively. Densitometry was used to quantify the blots, and each fraction was calculated and is represented here as percent of total (cytosolic + membrane). Results represent mean ± SE ($n \geq 3$). A representative blot is shown (C, M, and WCL indicate cytosolic fraction, membrane fraction, and whole cell lysates, respectively).

Figure 2

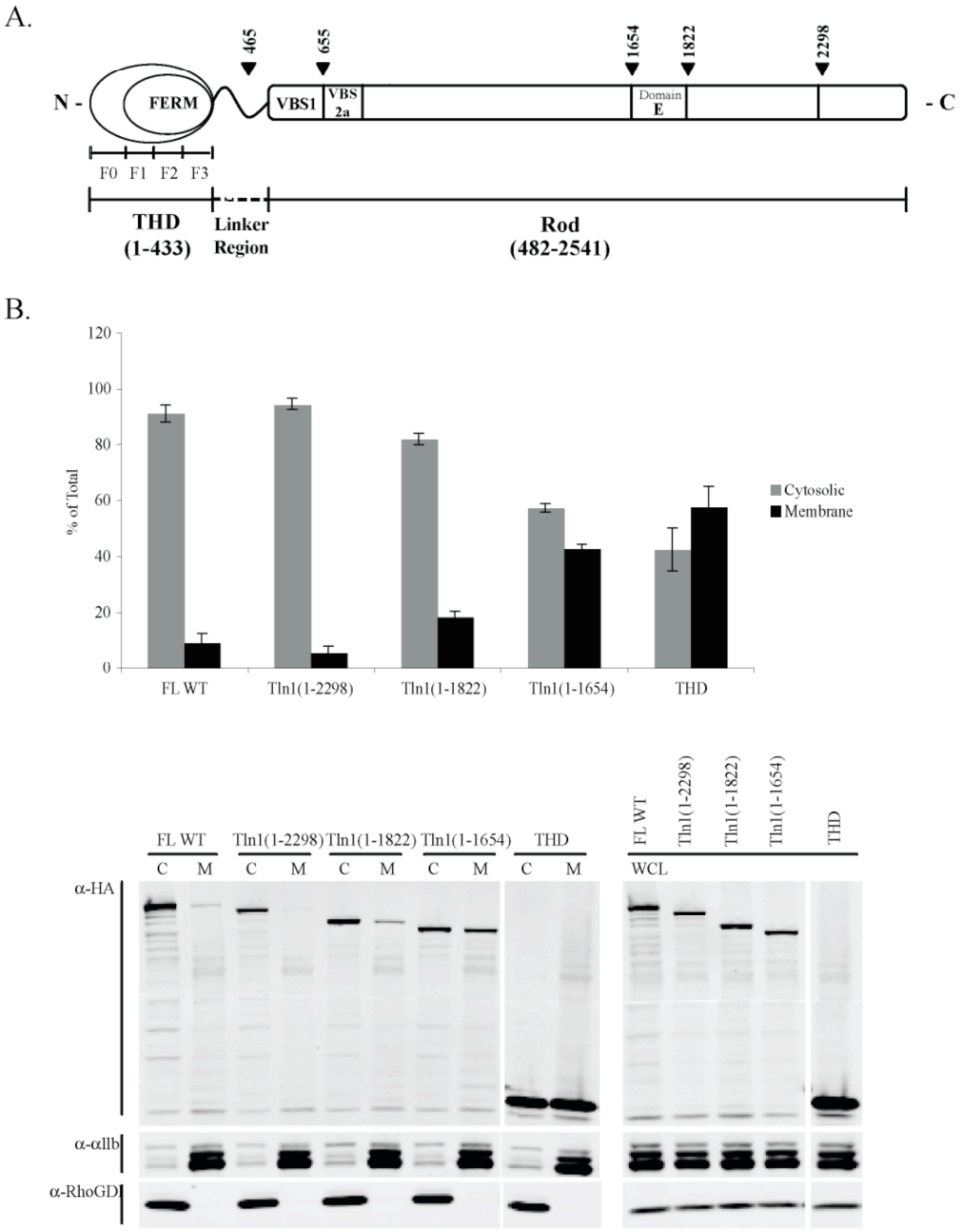
A.
465
655
1654
1822
2298
N -
FERM
VBS1
VBS 2a
Domain E
- C
F0 F1 F2 F3
THD (1-433)
Linker Region
Rod (482-2541)
B.
120
100
80
60
40
20
0
% of Total
Cytosolic
Membrane
FL WT
Tln1(1-2298)
Tln1(1-1822)
Tln1(1-1654)
THD
C M C M C M C M C M
WCL
α-HA
α-αIIb
α-RhoGDI

Figure 3

Deletion of Domain E increases membrane association of talin.

A. Schematic diagram of FL WT and FL talin mutant with Domain E deletion (FL ΔE). B. After 24 hour transfection, localization of FL WT, FL ΔE, or THD in A5 cells was assessed by subcellular fractionation, followed by western blotting with anti-HA antibody. Integrin αIIb and RhoGDI served as membrane and cytosolic markers, respectively. The blots were quantified with densitometric scanning, and each fraction was calculated and is represented here as percent of total (cytosolic + membrane). Results represent mean ± SE ($n \geq 3$). A representative blot is shown (C, M, and WCL represent cytosolic fraction, membrane fraction, and whole cell lysates, respectively).

Figure 3

A.

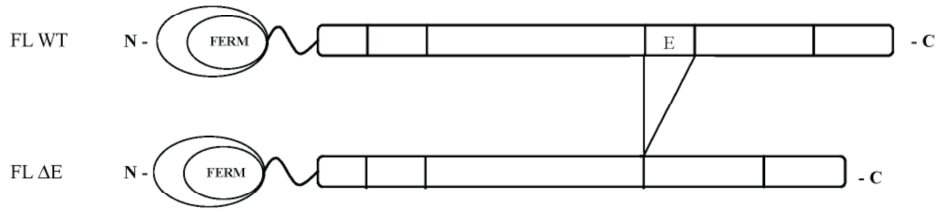
FL WT
N -
FERM
E
- C
FL ΔE
N -
FERM
- C

B.

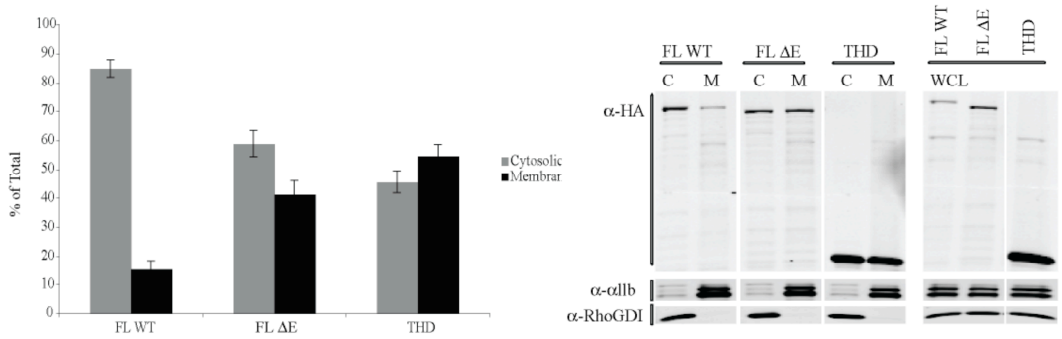
100
90
80
70
60
50
40
30
20
10
0
% of Total
FL WT
FL ΔE
THD
Cytosolic
Membrar
FL WT
FL ΔE
THD
C
M
C
M
C
M
WCL
α-HA
α-αIIb
α-RhoGDI

Figure 4

Domain E-F3 interaction prevents membrane association of talin.

A. Ribbon representation of the talin F3 (yellow) in complex with Domain E (green) (Protein Data Bank accession code 2KGX) (135). The residues in Domain E and those in the F3 domain that lie at the interacting interface are highlighted in red and blue, respectively: Asp1676, Asp1763, Glu1770, Glu1798, and Glu1805 in Domain E and Lys316, Lys318, Lys320, Lys322, Lys324, and Lys364 in the F3 domain. Met319 residue in the F3 domain reported to be involved in an intramolecular interaction of talin in Goksoy, *et al*. (134) is indicated in black. B. We mutated all of the residues in Domain E that are at the interface with the F3 to lysines (FL 5K) and examined localization of this mutant in A5 cells by subcellular fractionation followed by western blotting with anti-HA antibody. The blots were quantified with densitometric scanning, and each fraction was calculated and is represented here as percent of total (cytosolic + membrane). Results represent mean ± SE ($n \geq 3$). A representative blot is shown (C, M, and WCL represent cytosolic fraction, membrane fraction, and whole cell lysates, respectively). C. Localization of FL talin carrying an M319A point mutation (FL M319A) was also tested, as described above. Results represent mean ± SE ($n \geq 3$).

Figure 4

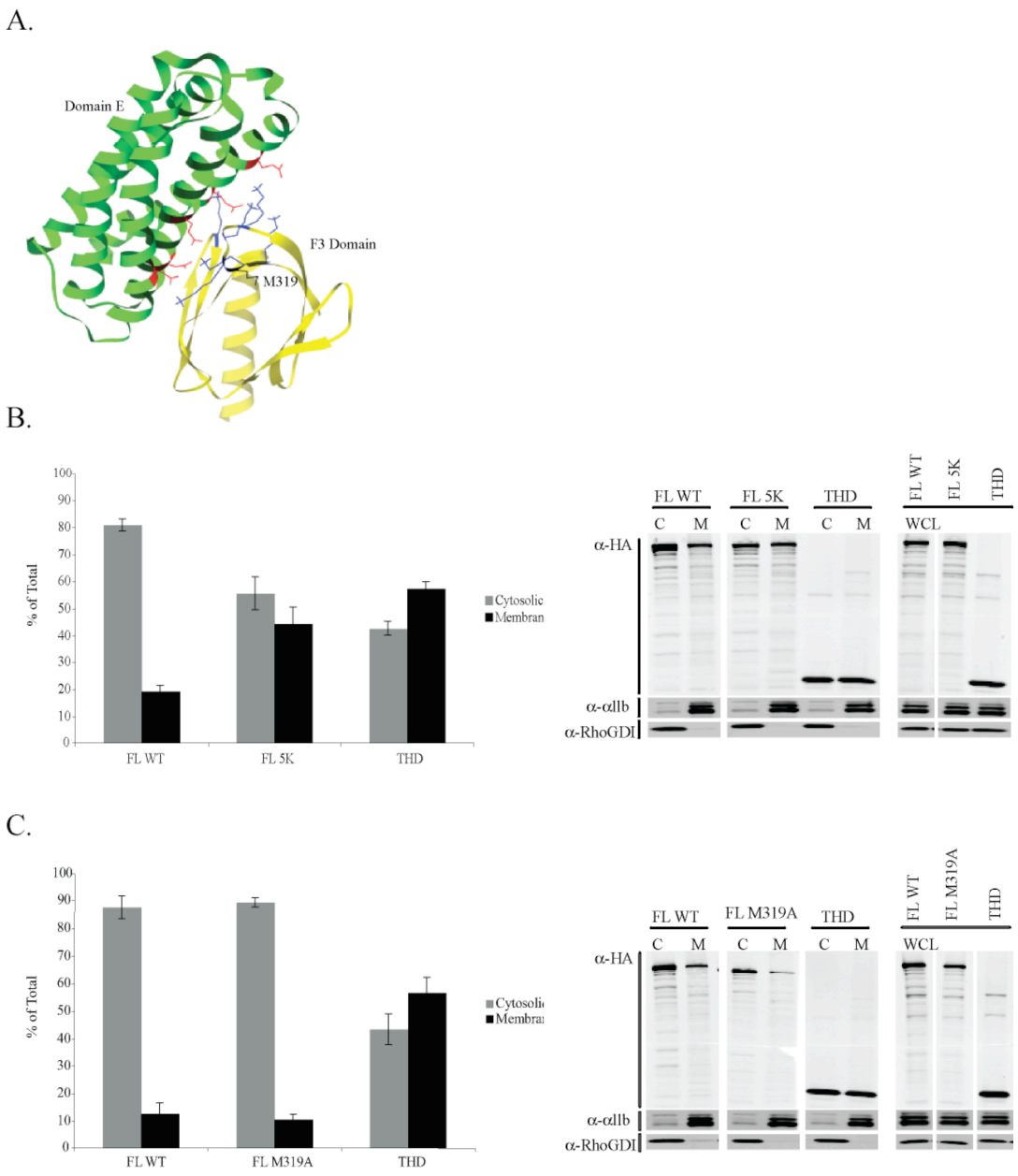
A.
Domain E
F3 Domain
M319
B.
% of Total
Cytosolic
Membran
FL WT
FL 5K
THD
C
M
WCL
α-HA
α-αIIb
α-RhoGDI
C.
% of Total
FL M319A

Figure 5

Disruption of Domain E-F3 interaction is insufficient for talin to activate αIIbβ3 integrins.

A5 cells were transfected with cDNAs encoding THD, FL WT, FL 5K, FL ΔE, FL M319A, or Tln1(1-1654) along with GFP (grey bars) or GFP-tagged RIAM176-CAAX (black bars). Twenty-four hours later, αIIbβ3 integrin activation was analyzed by flow cytometry using PAC1. The activation indices were calculated as described in "Methods" and are presented as percent increase over basal activation observed with empty pcDNA vector-transfected cells. Results represent mean ± SE ($n \geq 3$). Protein expression levels were verified by western blotting.

Figure 5

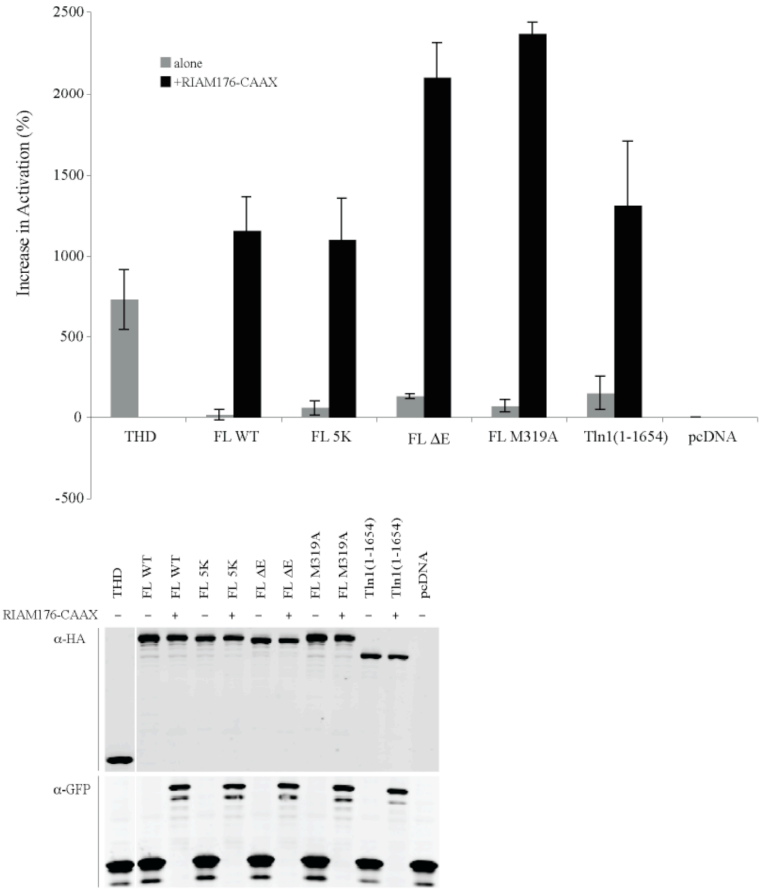
2500
2000
1500
1000
500
0
-500
Increase in Activation (%)
alone
+RIAM176-CAAX
THD
FL WT
FL 5K
FL ΔE
FL M319A
Tln1(1-1654)
pcDNA
THD
FL WT
FL WT
FL 5K
FL 5K
FL ΔE
FL ΔE
FL M319A
FL M319A
Tln1(1-1654)
Tln1(1-1654)
pcDNA
RIAM176-CAAX
α-HA
α-GFP

Figure 6

Disruption of Domain E-F3 interaction is insufficient for plasma membrane localization of talin.

After 24 hour transfection with THD or Tln1(1-1654), A5 cells were detached and subjected to surface biotinylation. Following subsequent fractionation of the surface-biotinylated cells, plasma membrane was isolated with streptavidin-conjugated magnetic beads. Distribution of the transfected talin was assessed by western blotting with anti-HA antibody. Endogenous FL-talin was detected with anti-talin antibody 8D4. Integrin αIIb, calnexin, lamin A/C, LAMP1, and RhoGDI served as the plasma membrane, ER membrane, nuclear membrane, lysosomal membrane, and cytsolic markers, respectively. A representative blot is shown (WCL, N/IC, C, CM, and PM indicate whole cell lysates, nuclear/intact cell, cytosolic, crude membrane, and plasma membrane fractions, respectively). Densitometry was used to quantify the blots, and talin in the plasma membrane fraction was calculated and is represented here as plasma membrane association. Bar graph represents mean ± SE ($n \geq 3$).

Figure 6

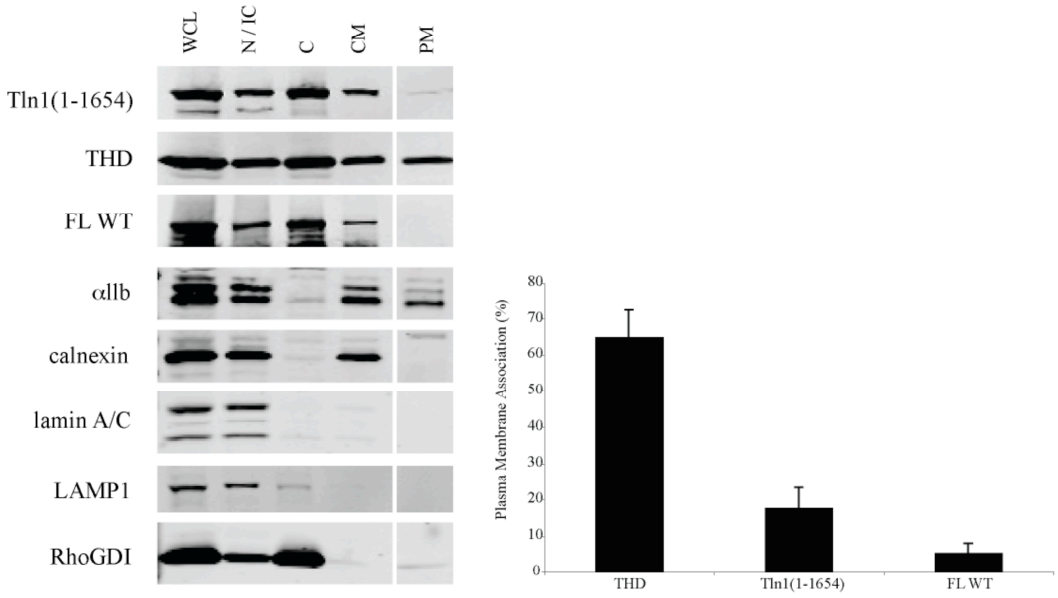
WCL
N / IC
C
CM
PM
Tln1(1-1654)
THD
FL WT
αIIb
calnexin
lamin A/C
LAMP1
RhoGDI
Plasma Membrane Association (%)
80
70
60
50
40
30
20
10
0
THD
Tln1(1-1654)
FL WT

Figure 7

Disruption of Domain E-F3 interaction is insufficient for talin to interact with integrin β3 cytoplasmic tails.

A. β3 integrins on A5 cells expressing THD, Tln1(1-1654), or FL WT were immunoprecipitated with anti-β3 mouse monoclonal antibody, and the bound talin was detected by western blotting with anti-HA antibody. β3 integrin capture was verified with anti-β3 rabbit polyclonal antibody. For each sample, the band corresponding to talin was quantified with densitometry and normalized by the respective input to account for the possible inequality in starting material. β3-dependent association is presented as percent of the maximal THD association. Data represent mean ± SE ($n \geq 3$). A representative blot is shown. B. His-Avi-tagged β3 or αIIb cytoplasmic tails captured on neutravidin beads were incubated with A5 cell lysates expressing THD, Tln1(1-1654), or FL WT. After overnight incubation, samples were washed and fractionated by SDS-PAGE. Bound talin was detected by western blotting with anti-HA antibody. For each sample, the band intensity was normalized by the respective input to account for the possible inequality in starting material. Coomassie staining verified the equal loading of β3 or αIIb cytoplasmic tails. Data are plotted as percent of the maximal THD binding and represent mean ± SE ($n \geq 3$). A representative blot is shown.

Figure 7

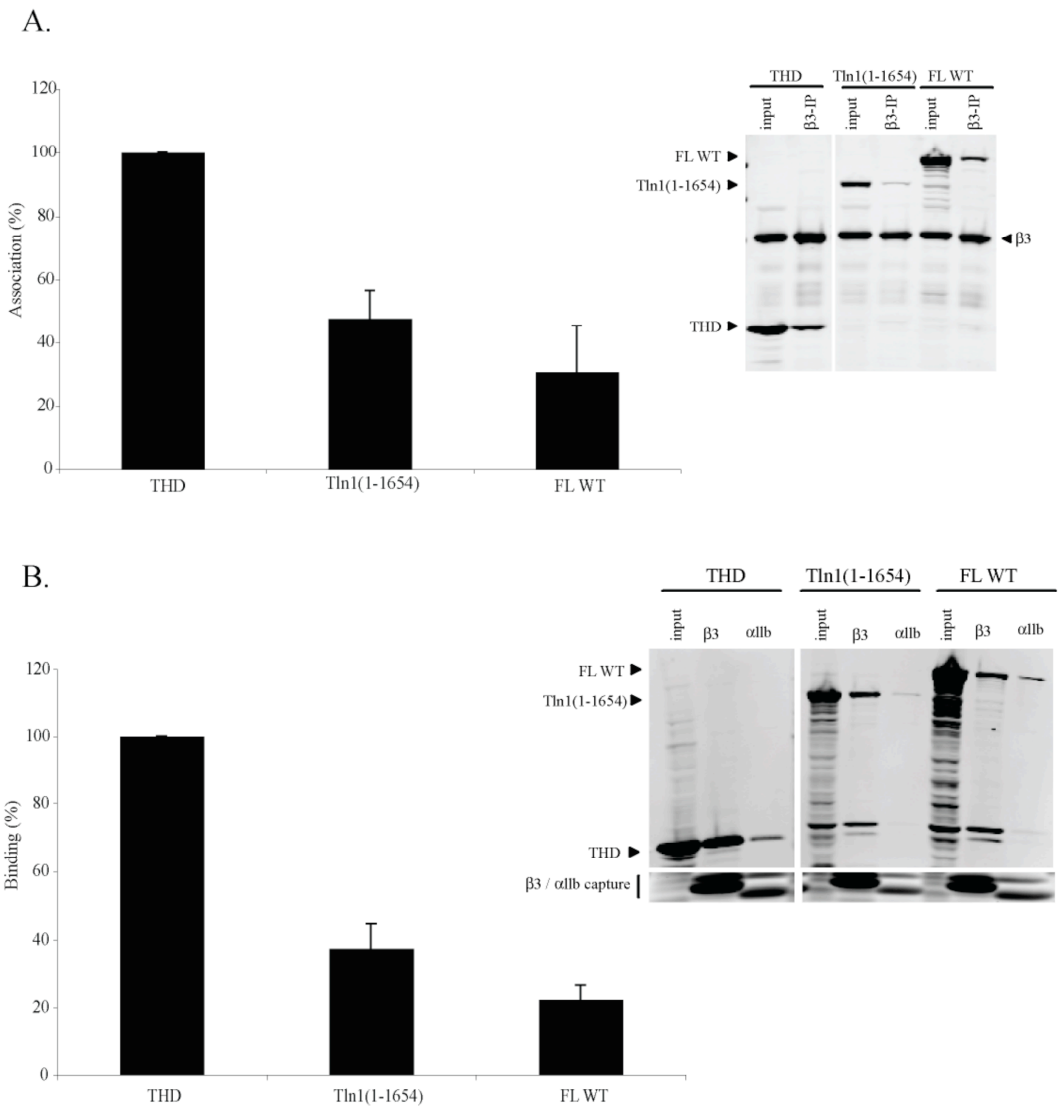
A.
Association (%)
120
100
80
60
40
20
0
THD
Tln1(1-1654)
FL WT
THD
Tln1(1-1654)
FL WT
input
β3-IP
input
β3-IP
input
β3-IP
FL WT
Tln1(1-1654)
β3
THD
B.
Binding (%)
120
100
80
60
40
20
0
THD
Tln1(1-1654)
FL WT
THD
Tln1(1-1654)
FL WT
input
β3
αIIb
input
β3
αIIb
input
β3
αIIb
FL WT
Tln1(1-1654)
THD
β3 / αIIb capture

Figure 8

Integrin binding is not necessary for plasma membrane localization.

After 24 hour transfection with THD or THD(R358,W359A), A5 cells were detached and subjected to surface biotinylation. Following subsequent fractionation of the surface-biotinylated cells, plasma membrane was isolated with streptavidin-conjugated magnetic beads. Distribution of the transfected talin was assessed by western blotting with anti-HA antibody. Endogenous FL-talin was detected with anti-talin antibody 8D4. Integrin αIIb, calnexin, lamin A/C, LAMP1, and RhoGDI served as the plasma membrane, ER membrane, nuclear membrane, lysosomal membrane, and cytsolic markers, respectively. A representative blot is shown (WCL, N/IC, C, CM, and PM indicate whole cell lysates, nuclear/intact cell, cytosolic, crude membrane, and plasma membrane fractions, respectively). Densitometry was used to quantify the blots, and talin in the plasma membrane fraction was calculated and is represented here as plasma membrane association. Bar graph represents mean ± SE ($n \geq 3$).

Figure 8

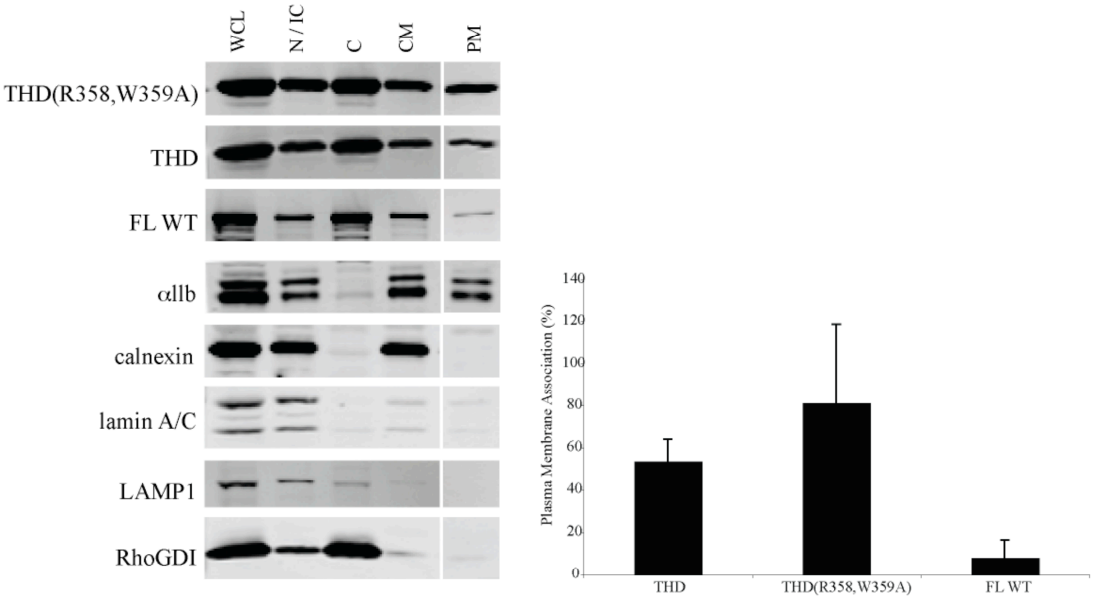
WCL
N / IC
C
CM
PM
THD(R358,W359A)
THD
FL WT
αIIb
calnexin
lamin A/C
LAMP1
RhoGDI
Plasma Membrane Association (%)
140
120
100
80
60
40
20
0
THD
THD(R358,W359A)
FL WT

Figure 9

Tln1(1-1654) does not activate nanodisc integrins as efficiently as THD.

Integrin-containing nanodiscs were incubated with increasing concentrations of purified recombinant THD (black) or Tln1(1-1654) (grey), and αIIbβ3 integrin activation was assessed by PAC1 binding. For each sample, data are plotted as percent increase over 0.0μM point in specific PAC1-binding. Graph shows mean ± SE of one representative experiment (three independent experiments were performed). SDS-PAGE shows the contents of integrin nanodiscs (αIIbβ3 integrins and MSP) and purified recombinant THD and Tln1(1-1654) used in the experiments.

Figure 9

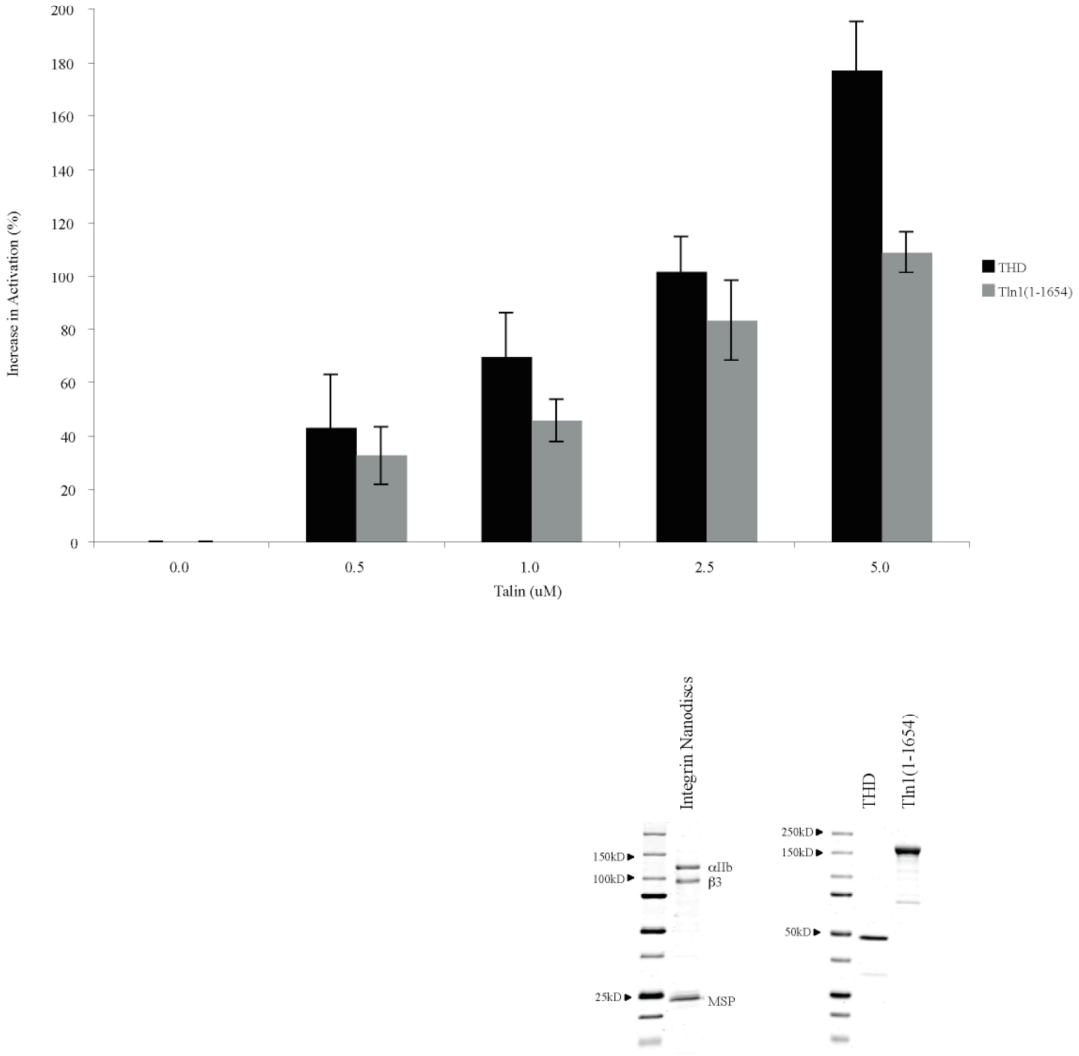
Increase in Activation (%)
200
180
160
140
120
100
80
60
40
20
0
0.0
0.5
1.0
2.5
5.0
Talin (uM)
THD
Tln1(1-1654)
Integrin Nanodiscs
150kD
100kD
25kD
αIIb
β3
MSP
THD
Tln1(1-1654)
250kD
150kD
50kD

Table 1

Summary of Interactions Between the Talin F23 Domain and the Rod Fragments. Presence or absence of inter-domain interaction was determined by collecting ^{15}N-HSQC spectra of ^{15}N-labelled F23 domain with and without increasing amounts of unlabelled talin fragments. The same ^{15}N-HSQC spectra collection was done for ^{15}N-labelled VBS1/2a domain. The ^{15}N-labelled components are shown in the row, and those unlabelled are in the columns. The experiments were performed by my collaborator Benjamin T. Goult (University of Leicester, UK).

Protein (aa)	**THD (1-433)**	**VBS1-2a-2b (434-911)**	**913-1653**	**1655-2294**	**2300-2541**
F23 (196-405)	Maybe	Yes	No	Yes	No
VBS1/2a (482-787)	Yes	No	No	No	No

Figure 10

VBS1/2a interacts with the F23 domain of talin.

A. $^{1}H,^{15}N$ HSQC spectra of 100 μM ^{15}N-labelled talin fragments were collected in the absence (green) or presence (blue) of unlabelled talin subdomain at ratio of 1:3 by my collaborator Benjamin T. Goult (University of Leicester, UK). B. Residues in the talin F23 domain (left) whose signals are affected by the addition of VBS1/2a highlighted in red in ribbon (top) and molecular surface (bottom) representation of the F23 domain. VBS1/2a residues (right) whose signals are perturbed following the addition of the talin F23 domain are highlighted in red in ribbon (top) and molecular surface (bottom) representation of VBS1/2a module.

Figure 10

A.

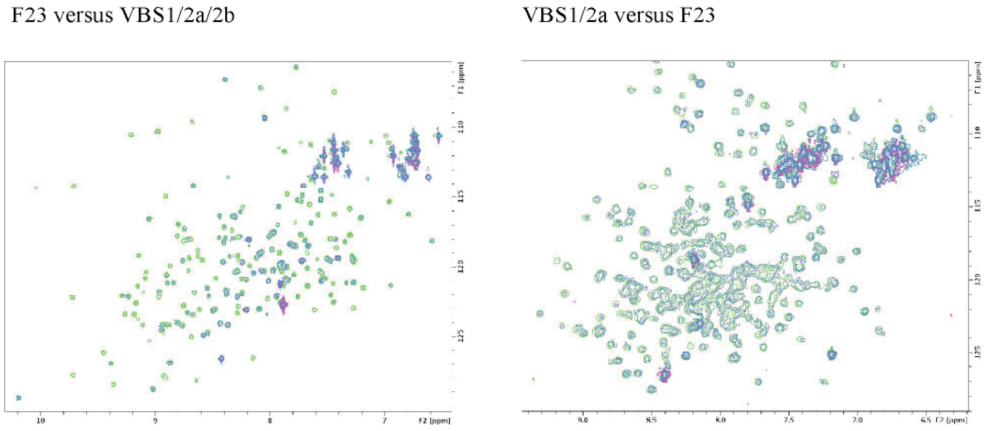

B.

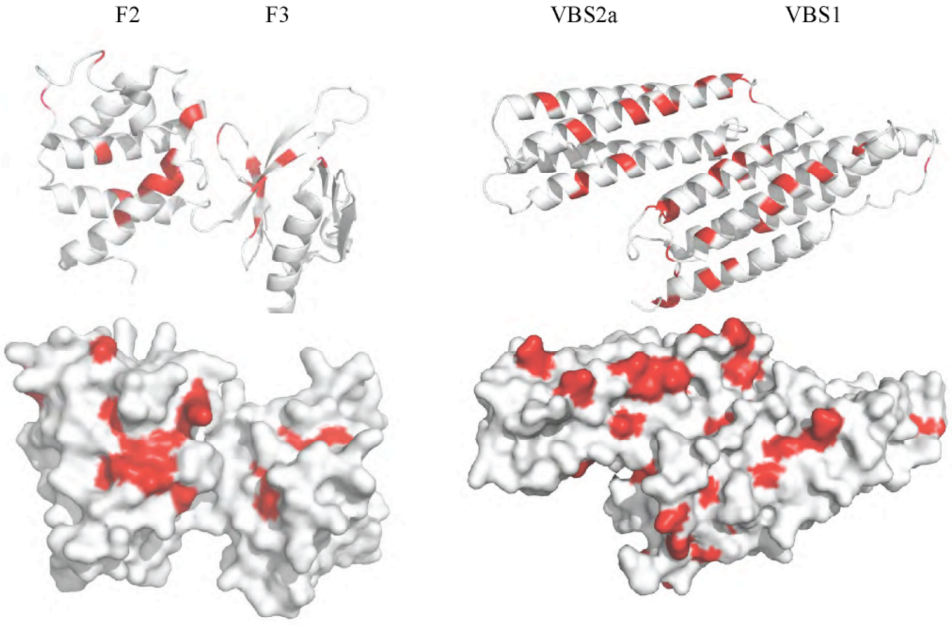

Figure 11

Truncation of VBS1/2a results in plasma membrane localization of talin.

After 24 hour transfection with THD, Tln1(1-465), Tln1(1-655) or Tln1(1-1654), A5 cells were detached and subjected to surface biotinylation. Following subsequent fractionation of the surface-biotinylated cells, plasma membrane was isolated with streptavidin-conjugated magnetic beads. Distribution of the transfected talin was assessed by western blotting with anti-HA antibody. Endogenous FL-talin was detected with anti-talin antibody 8D4. Integrin αIIb, calnexin, lamin A/C, LAMP1, and RhoGDI served as the plasma membrane, ER membrane, nuclear membrane, lysosomal membrane, and cytsolic markers, respectively. A representative blot is shown (WCL, N/IC, C, CM, and PM indicate whole cell lysates, nuclear/intact cell, cytosolic, crude membrane, and plasma membrane fractions, respectively). Densitometry was used to quantify the blots, and talin in the plasma membrane fraction was calculated and is represented here as plasma membrane association. Bar graph represents mean ± SE ($n \geq 3$).

Figure 11

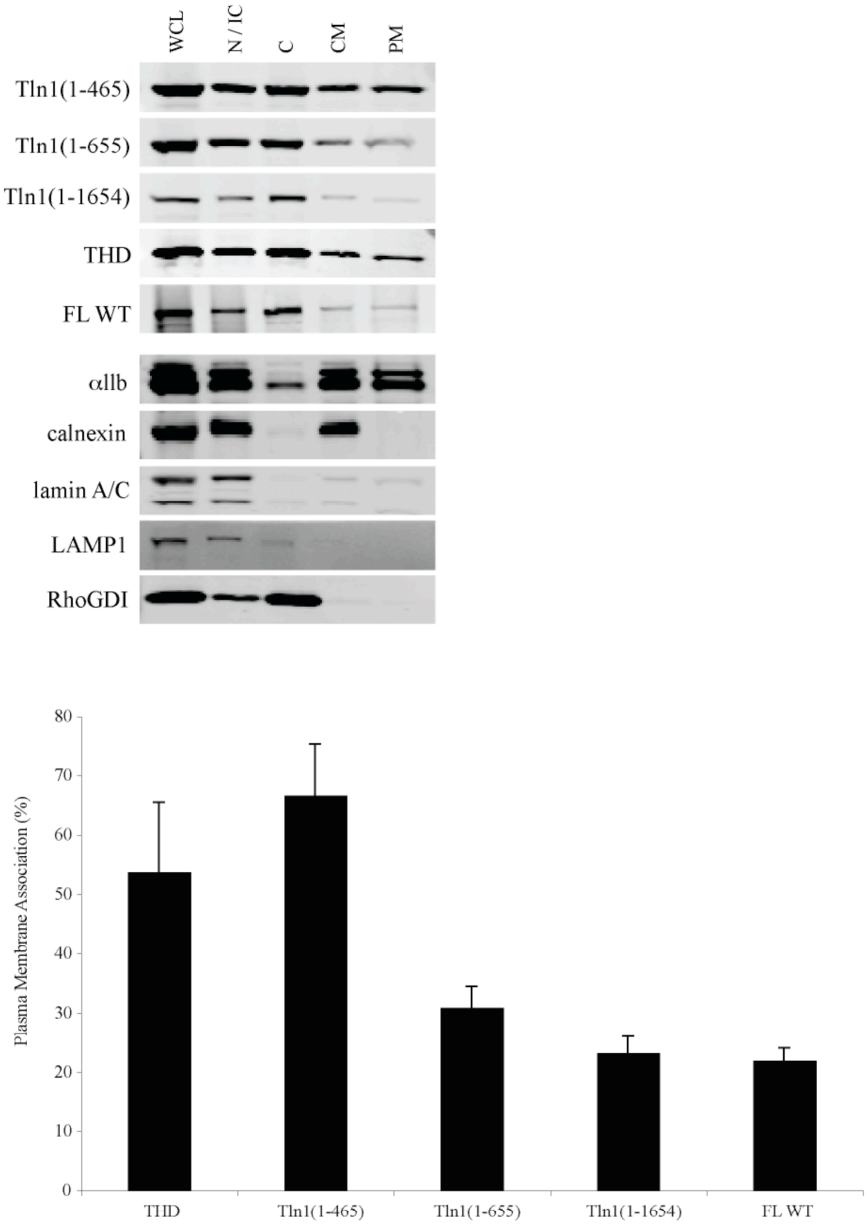
WCL
N / IC
C
CM
PM
Tln1(1-465)
Tln1(1-655)
Tln1(1-1654)
THD
FL WT
αIIb
calnexin
lamin A/C
LAMP1
RhoGDI
Plasma Membrane Association (%)
80
70
60
50
40
30
20
10
0
THD
Tln1(1-465)
Tln1(1-655)
Tln1(1-1654)
FL WT

Figure 12

Plasma membrane localization is insufficient for talin to activate αIIbβ3 integrins.

A. A5 cells were transfected with cDNAs encoding THD, Tln1(1-465), Tln1(1-1654) or FL WT. Twenty-four hours later, αIIbβ3 integrin activation was analyzed by flow cytometry using PAC1. The activation indices were calculated as described in "Methods" and are presented as percent increase over basal activation observed with empty pcDNA vector-transfected cells. Results represent mean ± SE (n ≥ 3). Protein expression levels were verified by western blotting. B. A5 cells were transfected with cDNAs encoding the talin F23 domain (Tln1(206-405)) or Tln1(206-450) along with GFP as transfection marker. Twenty-four hours later, αIIbβ3 integrin activation was analyzed by flow cytometry using PAC1. The activation indices were calculated as described in "Methods" and are presented as percent increase over basal activation observed with empty pcDNA vector-transfected cells. Results represent mean ± SE (n ≥ 3). Protein expression levels were verified by western blotting. Schematic diagram of the talin F23 domain and F23 domain with the extension of aa434-450 (Tln1(206-450)) is also shown.

Figure 12

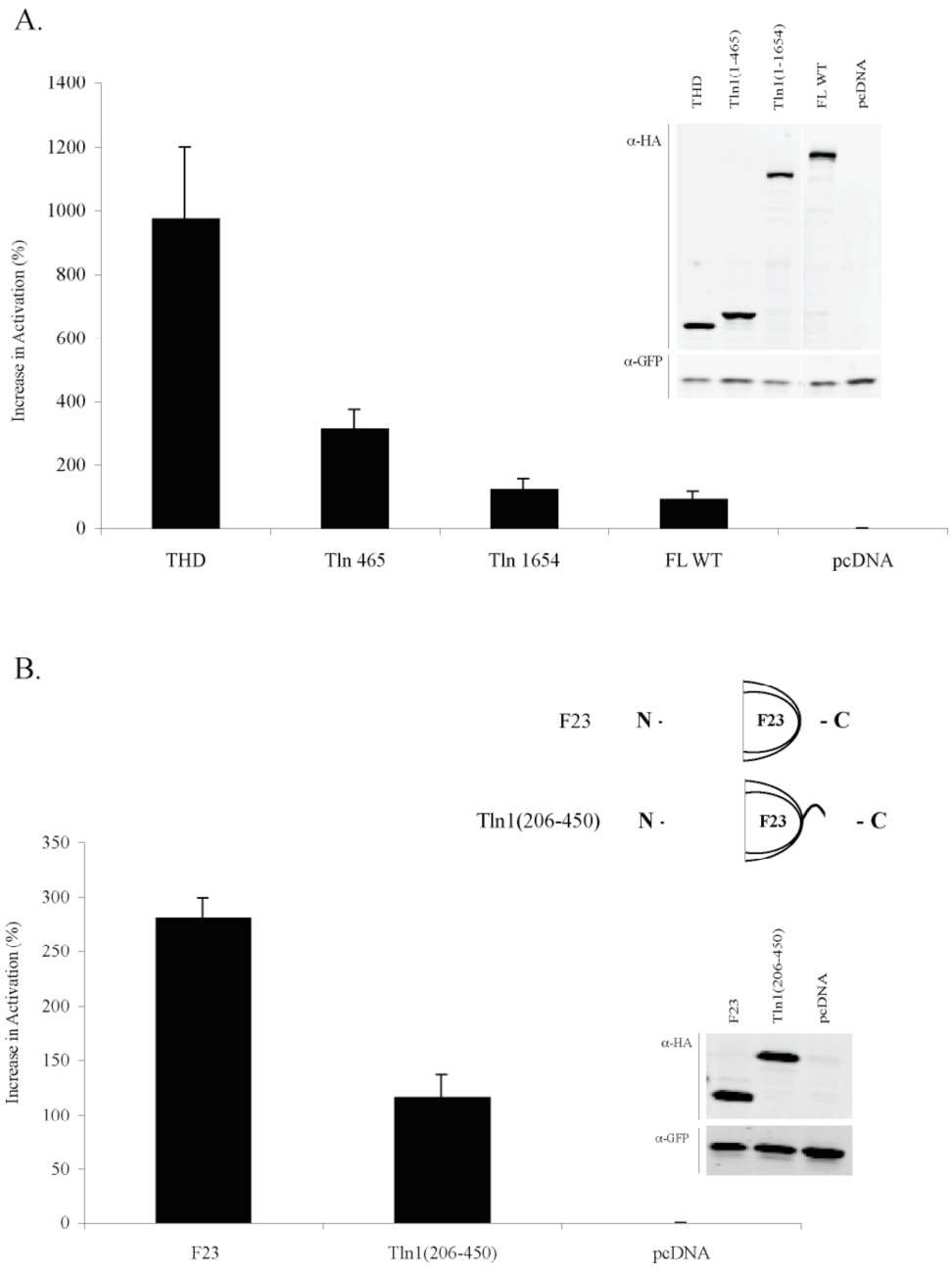
A.
Increase in Activation (%)
1400
1200
1000
800
600
400
200
0
THD
Tln 465
Tln 1654
FL WT
pcDNA
THD
Tln1(1-465)
Tln1(1-1654)
FL WT
pcDNA
α-HA
α-GFP
B.
F23 N - F23 - C
Tln1(206-450) N - F23 - C
Increase in Activation (%)
350
300
250
200
150
100
50
0
F23
Tln1(206-450)
pcDNA
F23
Tln1(206-450)
pcDNA
α-HA
α-GFP

Figure 13

The aa434-450 fragment can interfere with THD-mediated integrin activation in *trans*.

A. GFP-434-450 or GFP-Scr were co-transfected with THD in A5 cells. Twenty-four hours later, αIIbβ3 integrin activation level was examined by measuring PAC1 binding. The activation indices were calculated as described in "Methods". Then, results are presented as percent inhibition in activation, relative to GFP-only co-transfected cells and represent mean ± SE ($n \geq 3$). Protein expression was verified by western blotting. B. The effects of GFP-434-450 and GFP-470-486 (an irrelevant same-length fragment of talin) on THD mediated αIIbβ3 integrin activation were compared.

Figure 13

A.

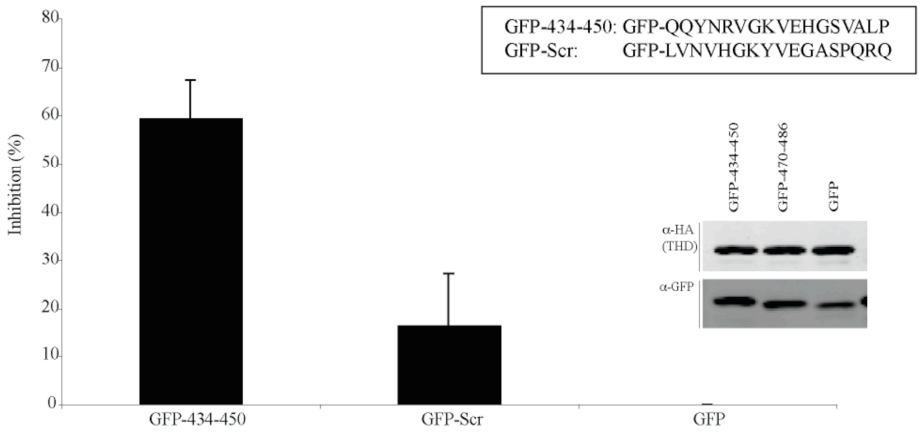
GFP-434-450: GFP-QQYNRVGKVEHGSVALP
GFP-Scr: GFP-LVNVHGKYVEGASPQRQ
Inhibition (%)
80
70
60
50
40
30
20
10
0
GFP-434-450
GFP-Scr
GFP
GFP-434-450
GFP-470-486
GFP
α-HA (THD)
α-GFP

B.

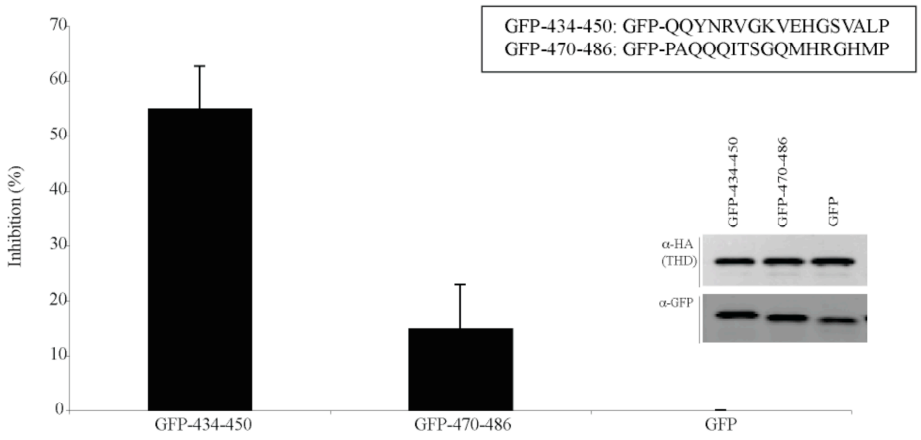
GFP-434-450: GFP-QQYNRVGKVEHGSVALP
GFP-470-486: GFP-PAQQQITSGQMHRGHMP
Inhibition (%)
70
60
50
40
30
20
10
0
GFP-434-450
GFP-470-486
GFP
GFP-434-450
GFP-470-486
GFP
α-HA (THD)
α-GFP

Figure 14

The aa434-450 fragment interferes with the interaction of talin with the β3 cytoplasmic tails.

His-Avi-tagged β3 cytoplasmic tails captured on neutravidin beads were mixed with increasing amounts of purified recombinant His-tagged THD or Tln1(1-465). After overnight incubation, samples were washed and fractionated by SDS-PAGE. Bound talin was detected by western blotting anti-His antibody. The bands were quantified with densitometry, which was normalized by the corresponding input to adjust for the possible inequality in starting material between THD and Tln1(1-465). Coomassie staining verified the equal loading of β3 cytoplasmic tails. Data are plotted as percent of the maximal THD binding and represent mean ± SE ($n \geq 3$). A representative blot is shown.

Figure 14

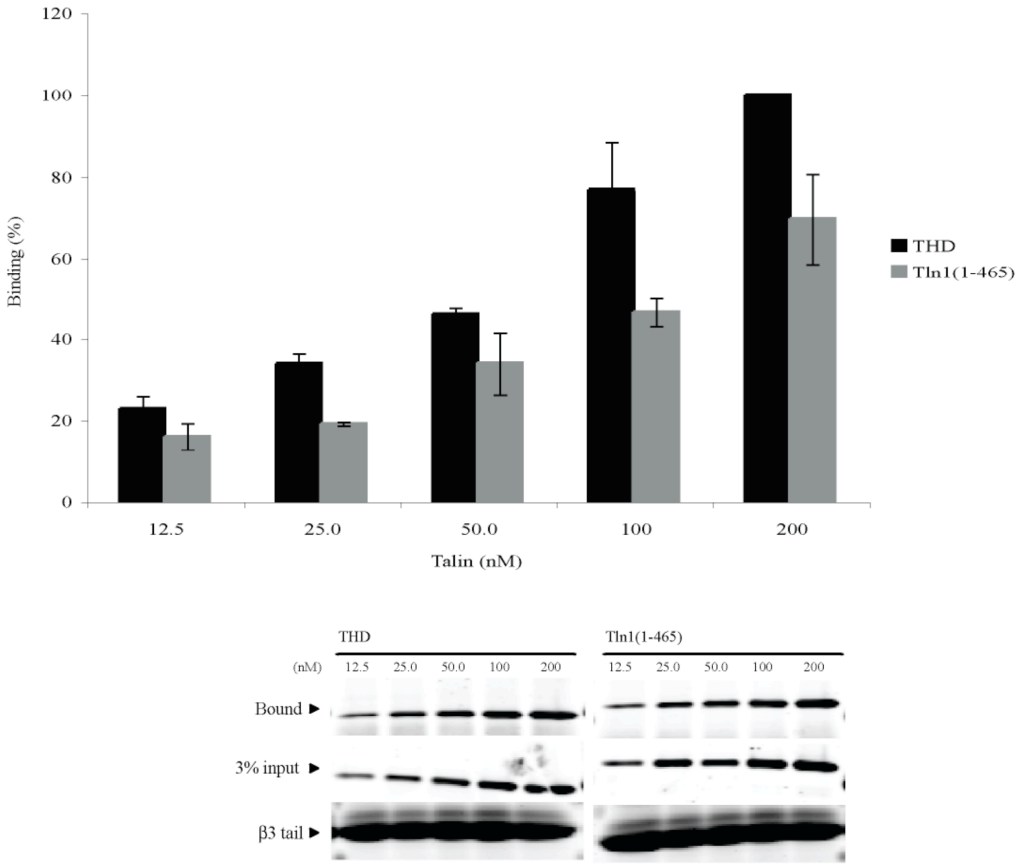
120
100
80
60
40
20
0
Binding (%)
12.5
25.0
50.0
100
200
Talin (nM)
THD
Tln1(1-465)
THD
Tln1(1-465)
(nM)
12.5
25.0
50.0
100
200
12.5
25.0
50.0
100
200
Bound ▶
3% input ▶
β3 tail ▶

Figure 15

The aa434-450 fragment has the inhibitory effect in *in-vitro* nanodisc system.

A. Integrin-containing nanodiscs were incubated with increasing concentrations of purified recombinant THD (black) or Tln1(1-465) (grey), and αIIbβ3 integrin activation was assessed by PAC1 binding. For each sample, data are plotted as percent increase over 0.0μM point in specific PAC1-binding. Graph shows mean ± SE of one representative experiment (three independent experiments were performed). SDS-PAGE shows the contents of integrin nanodiscs (αIIbβ3 integrins and MSP) and purified recombinant THD and Tln1(1-465) used in the experiments. B. 5.0uM of His-tagged THD was mixed with 0.1uM of GST-434-450, GST-Scr, or GST, which was then incubated with Integrin nanodiscs. Integrin activation was assessed by PAC1 binding. Results are presented as percent inhibition in activation, relative to GST-only condition, and represent mean ± SE ($n \geq 3$).

Figure 15

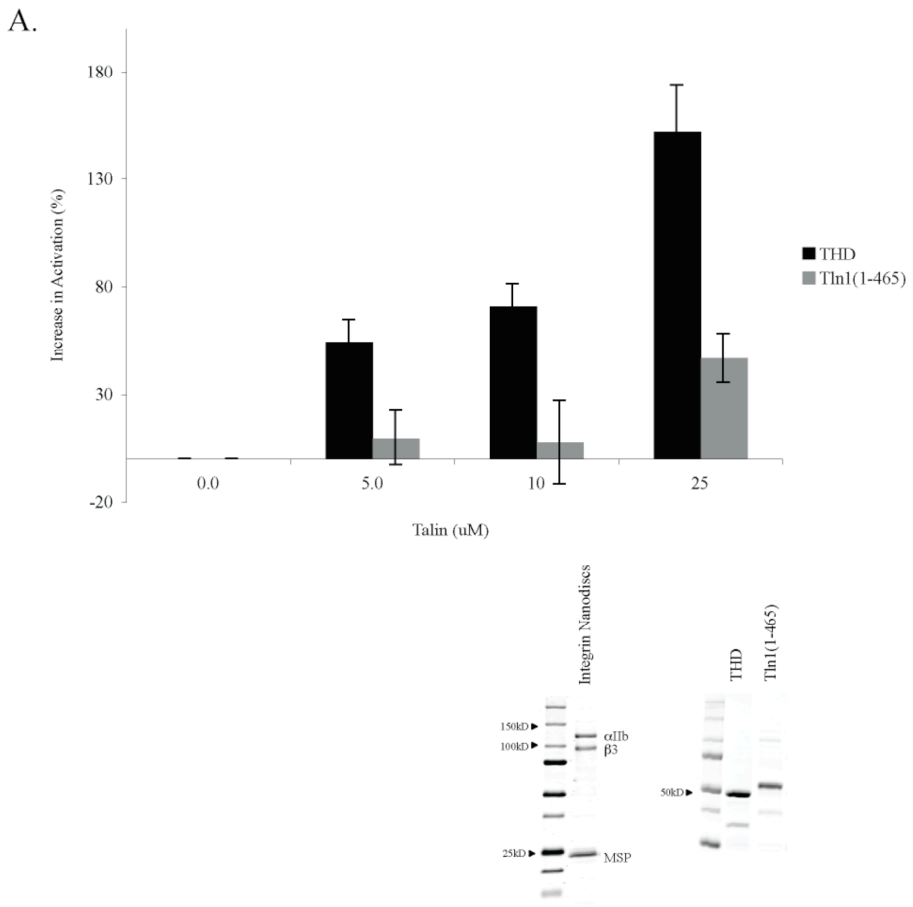
A.
180
130
80
30
-20
Increase in Activation (%)
0.0
5.0
10
25
Talin (uM)
THD
Tln1(1-465)
Integrin Nanodiscs
150kD
100kD
αIIb
β3
25kD
MSP
THD
Tln1(1-465)
50kD

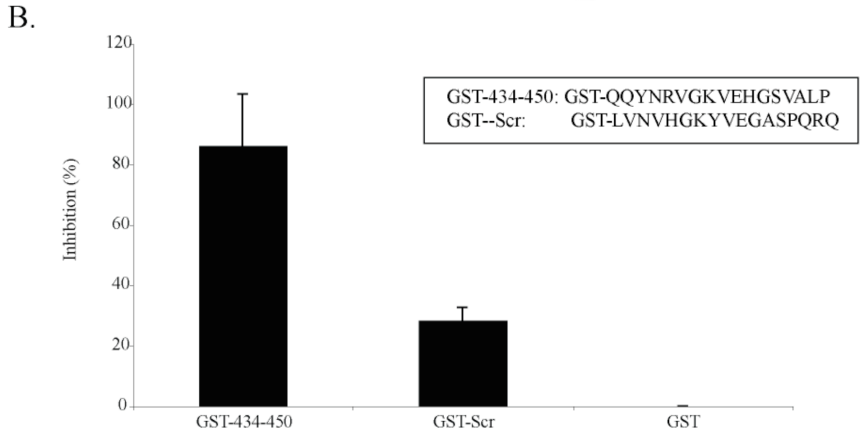
B.
120
100
80
60
40
20
0
Inhibition (%)
GST-434-450: GST-QQYNRVGKVEHGSVALP
GST--Scr: GST-LVNVHGKYVEGASPQRQ
GST-434-450
GST-Scr
GST

Figure 16

Non-inhibitory α-helical module prevents THD-mediated integrin activation.

A. A5 cells were transfected with cDNAs encoding THD, FL WT, or FL5K Δ434-912 along with GFP. Twenty-four hours later, αIIbβ3 integrin activation was analyzed by flow cytometry using PAC1. The activation indices were calculated as described in "Methods" and are presented as percent increase over basal activation observed with empty pcDNA vector-transfected cells. Results represent mean ± SE ($n \geq 3$). Protein expression levels were verified by western blotting. B. A5 cells were transfected with cDNAs encoding THD, FL WT, or THD+1823-1654 along with GFP. Twenty-four hours later, αIIbβ3 integrin activation was analyzed by flow cytometry using PAC1. The activation indices were calculated as described in "Methods" and are presented as percent increase over basal activation observed with empty pcDNA vector-transfected cells. Results represent mean ± SE ($n \geq 3$). Protein expression levels were verified by western blotting.

Figure 16

A.

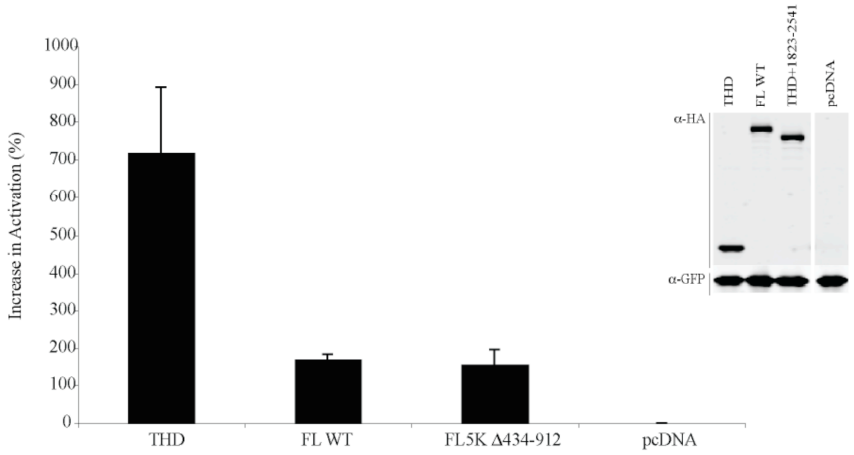
Increase in Activation (%)
1000
900
800
700
600
500
400
300
200
100
0
THD
FL WT
FL5K Δ434-912
pcDNA
THD
FL WT
THD+1823-2541
pcDNA
α-HA
α-GFP

B.

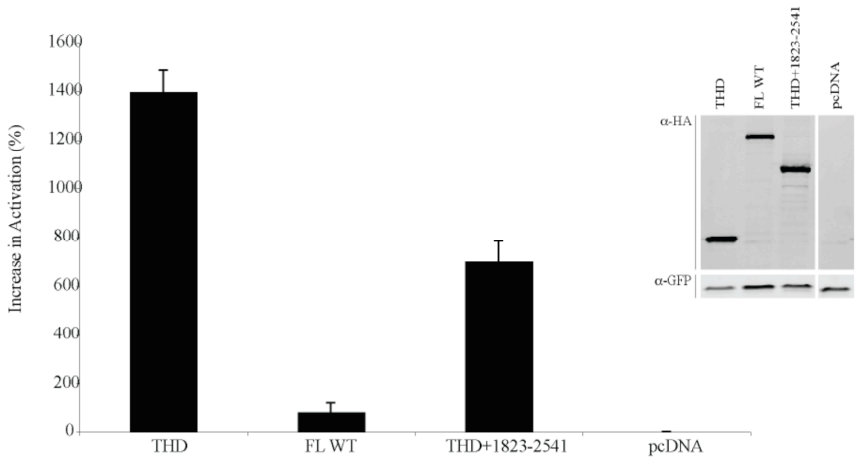
Increase in Activation (%)
1600
1400
1200
1000
800
600
400
200
0
THD
FL WT
THD+1823-2541
pcDNA
THD
FL WT
THD+1823-2541
pcDNA
α-HA
α-GFP

Figure 17

Talin contains three auto-inhibitory sites.

Schematic diagram of talin indicating three auto-inhibitory sites identified in this study: the aa434-450 fragment, VBS1/2a, and Domain E. The aa434-450 fragment interferes with the talin-integrin β tail interaction. VBS1/2a prevents plasma membrane localization of talin. Domain E keeps talin in the cytosol, and its deletion results in bulk membrane association of talin.

Figure 17

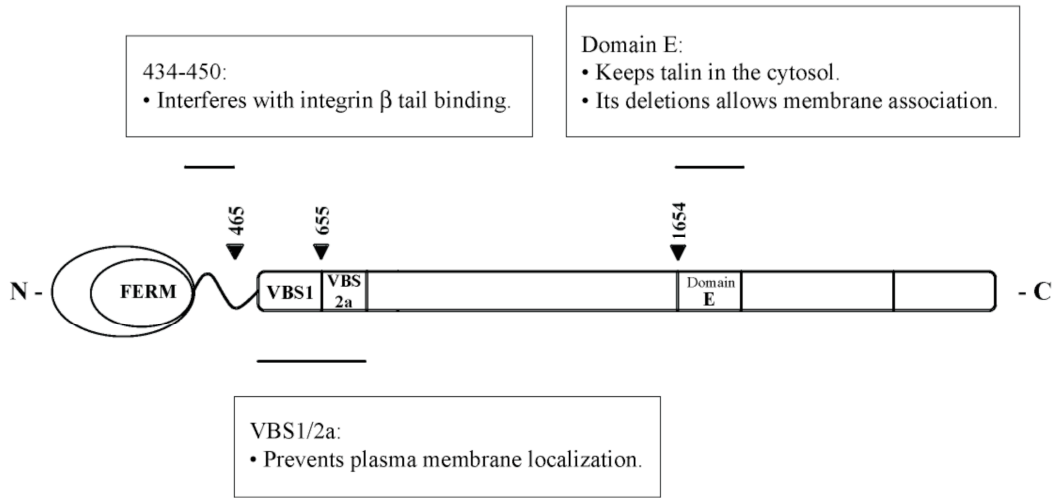
434-450:
• Interferes with integrin β tail binding.
Domain E:
• Keeps talin in the cytosol.
• Its deletions allows membrane association.
465
655
1654
N -
FERM
VBS1
VBS 2a
Domain E
- C
VBS1/2a:
• Prevents plasma membrane localization.

Chapter 4:

Discussion

Summary

Talin binding to the β cytoplasmic tails of integrins, following its translocation from the cytosol to the peripheral membrane (116,117,130,149), is necessary and sufficient for integrin activation (65,95-99). Yet, despite vigorous research and numerous reports, our understanding of how these functions of talin are regulated remains largely inconclusive.

Sequential C-terminal truncations of the talin rod domain and subsequent mutational analysis revealed that an α-helical bundle termed Domain E (134), located within aa1655-1822, negatively regulates membrane recruitment of talin via its inter-domain interaction with the F3 domain of talin. However, as we have shown both *in-vitro* and *in-vivo*, increased membrane association of talin caused by disruption of the Domain E-F3 interaction is insufficient for plasma membrane localization of talin, for the talin-integrin interaction, or for integrin activation. NMR analysis identified another inter-domain interaction between VBS1/2a module and the F23 domain of talin, and truncation of VBS1/2a resulted in plasma membrane localization of talin. In addition, a short fragment within the linker region between THD and the rod domain was identified that interferes with the talin-integrin interaction. Surprisingly, deletion of these auto-inhibitory sites from FL talin still fails to activate integrins, suggesting that the precise orientation of talin relative to the integrin tails and to the plasma

membrane may play an important role in the capacity of talin to activate integrins. In this study, we have mapped three auto-inhibitory sites within talin and have assigned a specific function to each one of them. These findings provide glimpses into the complexity of talin regulation.

Talin Domain E-F3 domain interactions negatively regulate its membrane recruitment. In support, disruption of the DomainE-F3 inter-domain interactions by deletion of or point mutations in Domain E increases membrane association to levels similar to what is observed with integrin-activating THD. Our results are consistent with previous studies; one of the residues in the F3 domain that interface with Domain E is Lys322 which is critical for talin membrane attachment and for integrin activation (80,99). Therefore, interaction with Domain E is consequently expected to mask this residue, hindering talin's association with membranes. Auto-inhibitory, intramolecular association between THD and the rod domain has been implicated in the regulation of talin activities (86,111,128,129), yet biological consequences of such interaction have remained elusive thus far. Here, we show that Domain E prevents membrane recruitment of talin by inter-domain interaction with the F3 domain of talin.

The association of talin with the membrane fraction observed by the disruption of Domain E-F3 interactions is insufficient to effect integrin activation, however; Tln1(1-1654), FL ΔE, and FL 5K which exhibit membrane recruitment comparable to that of THD fail to have proportional effects on αIIbβ3 integrin activation. It is unlikely that truncation, internal deletion, or point mutations affected

the overall structures of the resulting proteins and their abilities to activate integrins, for these talin mutants induce dramatic increase in integrin activation in the presence of RIAM176-CAAX that enhances talin-mediated integrin activation (116). Therefore, our observation that the deletion of Domain E and the disruption of the DomainE-F3 interaction fail to induce integrin activation strongly suggest that membrane-associated talin is regulated through additional mechanisms.

Domain E deletion is inadequate for plasma membrane targeting of talin. Although Tln1(1-1654) is found in the crude membrane fraction at levels nearly equivalent to THD, its presence in the purified plasma membrane fraction is markedly reduced compared to that of THD. In other words, the loss of Domain E allows bulk membrane association of talin, likely via unmasked Lys322 in the F3 domain, however it is insufficient to target talin specifically to the plasma membrane where integrins are expressed. This idea that the exposure of Lys322 alone is not sufficient for plasma membrane localization of talin is supported by the presence of lipid binding sites in other subdomains of THD that are also critical for integrin activation. In addition to Lys322 in the F3 domain (80), a region in the F1 domain (113) and a series of basic residues in the F2 domain, called the Membrane Orientation Patch (MOP) (112), are essential for the talin-membrane interaction and for integrin activation. Moreover, a recent structural study has revealed an open, extended conformation of THD that exposes all three lipid-binding sites (107). Therefore, it is reasonable to propose that additional membrane interactions via the F1 domain (113) and/or the MOP (112) are required for the effective localization of talin to the plasma membrane

and that these lipid binding sites remain somehow blocked in Tln1(1-1654). The cellular localization of Tln1(1-1654) (*e.g.* ER membrane, Golgi membrane, etc.) will need to be addressed by future investigations.

Tln1(1-1654) lacks ability to interact with αIIbβ3 integrins in cells, and this failure to associate with αIIbβ3 is ascribable to its reduced binding to the β3 integrin cytoplasmic tails. However, reduced binding to the β3 integrin cytoplasmic tails is not the reason for the failure to localize to the plasma membrane, as an integrin-binding defective THD mutant, THD(R358,W359A) (109), associated with the plasma membrane fraction similarly to WT THD. This is consistent with a previous study showing that re-distribution of talin to the plasma membrane following thrombin-activation is identical in normal and the αIIbβ3 integrin-null platelets (149). Furthermore, plasma membrane localization in itself is not sufficient to promote the talin-integrin interactions, as Tln1(1-1654) does not activate integrins as effectively as THD in an integrin nanodisc assay, which mimics a situation where talin is in close proximity to integrins at the plasma membrane. These findings together suggest that Tln1(1-1654) is defective in two functions, plasma membrane localization and integrin binding, and that additional inhibitory sites exist within aa434-1654. Indeed, other FERM domain-containing proteins are also regulated in their subcellular localization and substrate binding activities (132), hinting at a similar mode of regulation for talin.

The results from integrin nanodisc experiments imply that the additional mechanisms that regulate Tln1(1-1654) probably do not require extrinsic factors, since this *in-vitro* system that contains only purified αIIbβ3 integrins inserted into

membrane-like nanodiscs and purified recombinant talin eliminates the potential contributions of unknown cellular components and processes (99). Therefore, the additional mechanisms that inhibit the activities of Tln1(1-1654) do not likely involve other proteins or post-translational modifications of talin or integrins. This is not to say that Tln1(1-1654) does not require post-translational modification or interactions with lipids or an activating protein to become fully competent in its functions. In fact, this is a possibility that could be explored in future experiments.

There are reports proposing that auto-inhibition of talin can be released by calpain-mediated proteolytic cleavage (129,135) or by phosphotidylinositol 4,5-biphosphate binding (128,133). However, the relative roles of these processes in the regulation of talin and in physiological integrin activation await further investigation. The phosphorylation sites have also been mapped in talin isolated from activated human platelets (155). Moreover, Ser/Thr phosphorylation of talin has been shown to increase in thrombin-activated human platelets, although it is inadequate for plasma membrane localization of talin (149). In the case of ERM proteins, Thr phosphorylation is involved in their activation (156-158). Yet, again, the significance of talin phosphorylation in the context of integrin activation has yet to be realized.

THD-talin rod domain interaction was also reported by Goksoy, *et al* (133). In this study, the authors concluded that a single M319A point mutation in the F3 domain disrupts this inter-domain interaction, causing constitutive activation of talin and thereby inducing integrin activation (133). However, our examination of FL M319A localization by subcellular fractionation showed that FL M319A is mostly cytosolic.

Furthermore, in our hands, FL M319A does not induce integrin activation. These data indicate that Met319 does not play a direct role in talin membrane attachment or talin-mediated integrin activation. Our observations are in agreement with Goult. *et al*. who reported that Met319 is not directly involved in the Domain E-F3 interaction and that the M319A mutation does not have a significant effect on this inter-domain association (134). Together, these results suggest that a single point mutation is unlikely to release auto-inhibition of talin completely, especially in the context of FL talin. Consistent with this concept, when we tested the Domain E mutations individually in FL talin, none of the single point mutation increased membrane recruitment or integrin activation (data not shown). In sum, questions of how inhibitions on talin are released remain largely unanswered.

NMR analysis revealed another inter-domain interaction between VBS1/2a protein module and the F23 domain of talin. Truncation of VBS1/2a increases the abundance of talin in the plasma membrane fraction, suggesting that this domain is the negative regulator of plasma membrane localization of talin. As noted earlier, the F23 contains the MOP, and one of the F23 residues predicted to interface with VBS1/2a is important in the lipid binding of talin (112). Therefore, masking of one or more of those MOP residues by the interaction with VBS1/2a might interfere with efficient plasma membrane localization of talin. Furthermore, the involvement of the F23 domain agrees with observations by others that the N-terminus of THD cooperates with the F3 domain in integrin activation (111). It also supports our earlier

extrapolation that the exposure of more than one lipid binding site in THD might be required for talin to localize to the plasma membrane efficiently.

The role of the VBS1/2a-F23 interaction as a specific inhibitor of talin plasma membrane localization awaits further verification. For example, once we map the potential interacting residues, we can use this information to design mutations in VBS1/2a to try and disrupt this interaction. Such mutants will allow us to examine if disruption of this second inter-domain association would result in plasma membrane localization of talin. Moreover, identification of specific residues within the F23 domain that are involved in this interaction would likely provide insights as to what is required for talin to reach the plasma membrane.

Even in the absence of Domain E and VBS1/2a, plasma membrane localized talin fails to activate integrins. This is due to the short aa434-450 fragment that prevents talin from interacting with the integrin β3 cytoplasmic tails (Fig.14 and 15). Despite the convincing data supporting the specific, inhibitory role of the aa434-450 fragment on talin-mediated integrin activation, the current study has not elucidated the mechanism by which this short peptide interferes with the talin-integrin interaction. Nevertheless, the importance of inter-domain linker regions has been implicated for regulatory mechanisms involving conformational changes (159). Future biochemical and structural analyses, for instance, defining the interaction between THD and the aa434-450 fragment, should provide insights into the molecular basis of the aa434-450 fragment-mediated inhibition on talin.

Finally, in addition to specific inhibitions by Domain E, VBS1/2a, and the aa434-450 fragment, steric hindrance may also play a role in the regulation of talin functions. This is based on our data that the attachment of the α-helical bundles located within aa1823-2541 suppresses THD-mediated integrin activation. Our rationale here was that, if inhibitions on talin were solely mediated by mechanisms involving specific sequences, a protein module whose truncation exhibits no effect on subcellular localization of or integrin activation by talin would not affect the capacity of THD to activate integrins. Of note, the aa1823-2541 fragment does contain a dimerization domain (160), and one may argue that attachment of this fragment results in parallel or anti-parallel dimerization of THD causing the masking of critical sites in THD. However, truncation of this dimerization domain had no influence on subcellular localization or integrin activation. Thus, we conclude that inhibitory effects of the aa1823-2541 attachment on THD-mediated integrin activation is unlikely attributable to its reported role in talin dimerization.

How could steric hindrance regulate functions of talin? As described throughout this study, talin requires integrin binding at two distinct regions on the integrin β cytoplasmic tails (80,81,94,109,110) and lipid binding via multiple sites within THD (80,107,112,113) in order to activate integrins. Involvement of multiple sites and interactions strongly implies that the capacity of talin to activate integrins may depend on its precise orientation relative to integrins and the plasma membrane. Thus, we reason that steric hindrance can prevent talin from activating integrins in a non-specific fashion possibly by interfering with the exact positioning of THD

required for integrin activation. It would be interesting to test whether any bulky protein module could interfere with the precise orientation of talin and inhibit integrin activation.

Questions for Future Investigations

The significance of RIAM and Kindlins in talin-mediated integrin activation is unquestionable. Yet, many questions, some of which are discussed below, remain as to how these two proteins interplay with talin in integrin activation and need to be addressed by future molecular and structural studies.

RIAM complexed with Rap1 GTPase binds to and recruits talin to the plasma membrane and promotes talin-dependent integrin activation (86,116,117), suggesting that RIAM is capable of completely removing the inhibitions on talin. However, as our findings in this study suggest, plasma membrane localization is insufficient for talin to associate with and activate integrins, implying that the effect of RIAM is multifaceted. Then, what other consequences does RIAM binding to talin have besides plasma membrane recruitment? Another urgent question is the molecular mechanism underlying RIAM-mediated release of talin inhibition. Does RIAM binding to talin compete off auto-inhibitory inter-domain interactions, thereby exposing lipid binding and/or integrin binding sites of talin? By binding to the rod domain of talin, can RIAM physically take away the steric hindrance so that THD would be in the most optimal position to activate integrins?

There is ample evidence supporting the key role of kindlins in talin-mediated integrin activation. However, the synergistic effects of talin and kindlins appear to vary depending on the cellular system (124). What is the basis of cell type-, isoform-, and integrin-specificity? Moreover, understanding the precise relationship between talin and kindlins during integrin activation is imperative; do kindlins co-activate integrins by assisting talin in plasma membrane localization and/or integrin binding? Alternatively, kindlins may possibly be involved in a post-integrin binding event that has yet to be identified. Because kindlins and talin have not been reported to directly interact with each other, it is not unreasonable to speculate that functions of kindlins may involve another protein and/or post-translational modifications of talin or integrins. Finally, equally intriguing is the question of how RIAM and kindlins intersect during talin-mediated integrin activation.

Concluding Remarks

Integrin activation is implicated in a wide range of biological processes. Vigorous studies in the past two decades have produced an outstanding amount of knowledge about this signaling pathway, through application of genetics, biochemistry, cell, and structural biology. Especially, owning to the identification of central players and recent advances in the structural understanding of integrins and integrin tail-talin complex, we now have a clearer grasp of the final events of integrin activation. By focusing on talin, the pivot of integrin 'inside-out' signaling, and how its functions are regulated, this work has provided insights as to what happens to talin

during those final steps. Now, using the groundwork laid out by this study, future investigations may reveal how different signals converge on and activate talin, leading to integrin activation.

The text of Chapter 4, in part, is being prepared for publication. Asoka Banno, Benjamin T. Goult, Feng Ye, David R. Critchley, Mark H. Ginsberg. "Functional Mapping of Auto-Inhibitory Sites in Talin". I was the primary investigator of this research as well as the primary author of the manuscript.

Chapter 5:

References

1. Hynes, R. O. (2002) *Cell* **110**, 673-687

2. van der Flier, A., and Sonnenberg, A. (2001) *Cell Tissue Res* **305**, 285-298

3. Liddington, R. C., and Ginsberg, M. H. (2002) *J Cell Biol* **158**, 833-839

4. Williams, M. J., Hughes, P. E., O'Toole, T. E., and Ginsberg, M. H. (1994) *Trends Cell Biol* **4**, 109-112

5. Hynes, R. O. (1992) *Cell* **69**, 11-25

6. Tamkun, J. W., DeSimone, D. W., Fonda, D., Patel, R. S., Buck, C., Horwitz, A. F., and Hynes, R. O. (1986) *Cell* **46**, 271-282

7. Hynes, R. O. (1987) *Cell* **48**, 549-554

8. Kumar, C. C. (1998) *Oncogene* **17**, 1365-1373

9. Qin, J., Vinogradova, O., and Plow, E. F. (2004) *PLoS Biol* **2**, e169

10. Giancotti, F. G., and Ruoslahti, E. (1999) *Science* **285**, 1028-1032

11. Katsumi, A., Orr, A. W., Tzima, E., and Schwartz, M. A. (2004) *J Biol Chem* **279**, 12001-12004

12. Ingber, D. E. (1998) *Biol Bull* **194**, 323-325; discussion 325-327

13. Alenghat, F. J., and Ingber, D. E. (2002) *Sci STKE* **2002**, PE6

14. Ginsberg, M. H., Du, X., and Plow, E. F. (1992) *Curr Opin Cell Biol* **4**, 766-771

15. O'Toole, T. E., Mandelman, D., Forsyth, J., Shattil, S. J., Plow, E. F., and Ginsberg, M. H. (1991) *Science* **254**, 845-847

16. Hughes, P. E., Diaz-Gonzalez, F., Leong, L., Wu, C., McDonald, J. A., Shattil, S. J., and Ginsberg, M. H. (1996) *J Biol Chem* **271**, 6571-6574

17. Sims, P. J., Ginsberg, M. H., Plow, E. F., and Shattil, S. J. (1991) *J Biol Chem* **266**, 7345-7352

18. O'Toole, T. E., Loftus, J. C., Du, X. P., Glass, A. A., Ruggeri, Z. M., Shattil, S. J., Plow, E. F., and Ginsberg, M. H. (1990) *Cell Regul* **1**, 883-893

19. Legate, K. R., Wickstrom, S. A., and Fassler, R. (2009) *Genes Dev* **23**, 397-418

20. Koivunen, E., Ranta, T. M., Annila, A., Taube, S., Uppala, A., Jokinen, M., van Willigen, G., Ihanus, E., and Gahmberg, C. G. (2001) *J Cell Biol* **153**, 905-916

21. Li, Z. (1999) *Cell Res* **9**, 171-178

22. Semmrich, M., Smith, A., Feterowski, C., Beer, S., Engelhardt, B., Busch, D. H., Bartsch, B., Laschinger, M., Hogg, N., Pfeffer, K., and Holzmann, B. (2005) *J Exp Med* **201**, 1987-1998

23. Xiong, J. P., Stehle, T., Diefenbach, B., Zhang, R., Dunker, R., Scott, D. L., Joachimiak, A., Goodman, S. L., and Arnaout, M. A. (2001) *Science* **294**, 339-345

24. Arnaout, M. A., Goodman, S. L., and Xiong, J. P. (2007) *Curr Opin Cell Biol* **19**, 495-507

25. Askari, J. A., Buckley, P. A., Mould, A. P., and Humphries, M. J. (2009) *J Cell Sci* **122**, 165-170

26. Luo, B. H., Carman, C. V., and Springer, T. A. (2007) *Annu Rev Immunol* **25**, 619-647

27. Takagi, J., Petre, B. M., Walz, T., and Springer, T. A. (2002) *Cell* **110**, 599-611

28. Nishida, N., Xie, C., Shimaoka, M., Cheng, Y., Walz, T., and Springer, T. A. (2006) *Immunity* **25**, 583-594

29. Jin, M., Andricioaei, I., and Springer, T. A. (2004) *Structure* **12**, 2137-2147

30. Mould, A. P., and Humphries, M. J. (2004) *Curr Opin Cell Biol* **16**, 544-551

31. Zhu, J., Boylan, B., Luo, B. H., Newman, P. J., and Springer, T. A. (2007) *J Biol Chem* **282**, 11914-11920

32. Adair, B. D., Xiong, J. P., Maddock, C., Goodman, S. L., Arnaout, M. A., and Yeager, M. (2005) *J Cell Biol* **168**, 1109-1118

33. Xiong, J. P., Stehle, T., Goodman, S. L., and Arnaout, M. A. (2003) *Blood* **102**, 1155-1159

34. Shattil, S. J., Kim, C., and Ginsberg, M. H. (2010) *Nat Rev Mol Cell Biol* **11**, 288-300

35. Takagi, J., and Springer, T. A. (2002) *Immunol Rev* **186**, 141-163

36. Shimaoka, M., Takagi, J., and Springer, T. A. (2002) *Annu Rev Biophys Biomol Struct* **31**, 485-516

37. Carman, C. V., and Springer, T. A. (2003) *Curr Opin Cell Biol* **15**, 547-556

38. Bazzoni, G., and Hemler, M. E. (1998) *Trends Biochem Sci* **23**, 30-34

39. Hato, T., Pampori, N., and Shattil, S. J. (1998) *J Cell Biol* **141**, 1685-1695

40. Stefansson, A., Armulik, A., Nilsson, I., von Heijne, G., and Johansson, S. (2004) *J Biol Chem* **279**, 21200-21205

41. Gottschalk, K. E., Adams, P. D., Brunger, A. T., and Kessler, H. (2002) *Protein Sci* **11**, 1800-1812

42. Scott, J. P., 3rd, Scott, J. P., 2nd, Chao, Y. L., Newman, P. J., and Ward, C. M. (1998) *Thromb Haemost* **80**, 546-550

43. Nurden, A. T., Breillat, C., Jacquelin, B., Combrie, R., Freedman, J., Blanchette, V. S., Schmugge, M., and Rand, M. L. (2004) *J Thromb Haemost* **2**, 813-819

44. Partridge, A. W., Liu, S., Kim, S., Bowie, J. U., and Ginsberg, M. H. (2005) *J Biol Chem* **280**, 7294-7300

45. Lau, T. L., Kim, C., Ginsberg, M. H., and Ulmer, T. S. (2009) *Embo J* **28**, 1351-1361

46. Kim, C., Lau, T. L., Ulmer, T. S., and Ginsberg, M. H. (2009) *Blood* **113**, 4747-4753

47. Luo, B. H., Carman, C. V., Takagi, J., and Springer, T. A. (2005) *Proc Natl Acad Sci USA* **102**, 3679-3684

48. Li, W., Metcalf, D. G., Gorelik, R., Li, R., Mitra, N., Nanda, V., Law, P. B., Lear, J. D., Degrado, W. F., and Bennett, J. S. (2005) *Proc Natl Acad Sci U S A* **102**, 1424-1429

49. Luo, B. H., Springer, T. A., and Takagi, J. (2004) *PLoS Biol* **2**, e153

50. Calderwood, D. A. (2004) *J Cell Sci* **117**, 657-666

51. Hughes, P. E., O'Toole, T. E., Ylanne, J., Shattil, S. J., and Ginsberg, M. H. (1995) *J Biol Chem* **270**, 12411-12417

52. Iber, D., and Campbell, I. D. (2006) *Bull Math Biol* **68**, 945-956

53. Ma, Y. Q., Yang, J., Pesho, M. M., Vinogradova, O., Qin, J., and Plow, E. F. (2006) *Biochemistry* **45**, 6656-6662

54. O'Toole, T. E., Katagiri, Y., Faull, R. J., Peter, K., Tamura, R., Quaranta, V., Loftus, J. C., Shattil, S. J., and Ginsberg, M. H. (1994) *J Cell Biol* **124**, 1047-1059

55. Lu, C., Takagi, J., and Springer, T. A. (2001) *J Biol Chem* **276**, 14642-14648

56. Vinogradova, O., Velyvis, A., Velyviene, A., Hu, B., Haas, T., Plow, E., and Qin, J. (2002) *Cell* **110**, 587-597

57. Takagi, J., Erickson, H. P., and Springer, T. A. (2001) *Nat Struct Biol* **8**, 412-416

58. Kim, M., Carman, C. V., and Springer, T. A. (2003) *Science* **301**, 1720-1725

59. Ginsberg, M. H., Partridge, A., and Shattil, S. J. (2005) *Curr Opin Cell Biol* **17**, 509-516

60. O'Toole, T. E., Ylanne, J., and Culley, B. M. (1995) *J Biol Chem* **270**, 8553-8558

61. Ulmer, T. S., Yaspan, B., Ginsberg, M. H., and Campbell, I. D. (2001) *Biochemistry* **40**, 7498-7508

62. Wang, R., Shattil, S. J., Ambruso, D. R., and Newman, P. J. (1997) *J Clin Invest* **100**, 2393-2403

63. Liu, S., Calderwood, D. A., and Ginsberg, M. H. (2000) *J Cell Sci* **113 (Pt 20)**, 3563-3571

64. Zaidel-Bar, R., Itzkovitz, S., Ma'ayan, A., Iyengar, R., and Geiger, B. (2007) *Nat Cell Biol* **9**, 858-867

65. Tadokoro, S., Shattil, S. J., Eto, K., Tai, V., Liddington, R. C., de Pereda, J. M., Ginsberg, M. H., and Calderwood, D. A. (2003) *Science* **302**, 103-106

66. Horwitz, A., Duggan, K., Buck, C., Beckerle, M. C., and Burridge, K. (1986) *Nature* **320**, 531-533

67. Eigenthaler, M., Hofferer, L., Shattil, S. J., and Ginsberg, M. H. (1997) *J Biol Chem* **272**, 7693-7698

68. Kashiwagi, H., Schwartz, M. A., Eigenthaler, M., Davis, K. A., Ginsberg, M. H., and Shattil, S. J. (1997) *J Cell Biol* **137**, 1433-1443

69. Shattil, S. J., O'Toole, T., Eigenthaler, M., Thon, V., Williams, M., Babior, B. M., and Ginsberg, M. H. (1995) *J Cell Biol* **131**, 807-816

70. Kolanus, W., Nagel, W., Schiller, B., Zeitlmann, L., Godar, S., Stockinger, H., and Seed, B. (1996) *Cell* **86**, 233-242

71. Korthauer, U., Nagel, W., Davis, E. M., Le Beau, M. M., Menon, R. S., Mitchell, E. O., Kozak, C. A., Kolanus, W., and Bluestone, J. A. (2000) *J Immunol* **164**, 308-318

72. Yuan, W., Leisner, T. M., McFadden, A. W., Wang, Z., Larson, M. K., Clark, S., Boudignon-Proudhon, C., Lam, S. C., and Parise, L. V. (2006) *J Cell Biol* **172**, 169-175

73. Liu, S., Thomas, S. M., Woodside, D. G., Rose, D. M., Kiosses, W. B., Pfaff, M., and Ginsberg, M. H. (1999) *Nature* **402**, 676-681

74. Katagiri, K., Maeda, A., Shimonaka, M., and Kinashi, T. (2003) *Nat Immunol* **4**, 741-748

75. Tohyama, Y., Katagiri, K., Pardi, R., Lu, C., Springer, T. A., and Kinashi, T. (2003) *Mol Biol Cell* **14**, 2570-2582

76. Meves, A., Stremmel, C., Gottschalk, K., and Fassler, R. (2009) *Trends Cell Biol* **19**, 504-513

77. Oxley, C. L., Anthis, N. J., Lowe, E. D., Vakonakis, I., Campbell, I. D., and Wegener, K. L. (2008) *J Biol Chem* **283**, 5420-5426

78. Millon-Fremillon, A., Bouvard, D., Grichine, A., Manet-Dupe, S., Block, M. R., and Albiges-Rizo, C. (2008) *J Cell Biol* **180**, 427-441

79. Kiema, T., Lad, Y., Jiang, P., Oxley, C. L., Baldassarre, M., Wegener, K. L., Campbell, I. D., Ylanne, J., and Calderwood, D. A. (2006) *Mol Cell* **21**, 337-347

80. Wegener, K. L., Partridge, A. W., Han, J., Pickford, A. R., Liddington, R. C., Ginsberg, M. H., and Campbell, I. D. (2007) *Cell* **128**, 171-182

81. Calderwood, D. A., Fujioka, Y., de Pereda, J. M., Garcia-Alvarez, B., Nakamoto, T., Margolis, B., McGlade, C. J., Liddington, R. C., and Ginsberg, M. H. (2003) *Proc Natl Acad Sci U S A* **100**, 2272-2277

82. Kinbara, K., Goldfinger, L. E., Hansen, M., Chou, F. L., and Ginsberg, M. H. (2003) *Nat Rev Mol Cell Biol* **4**, 767-776

83. Hughes, P. E., Renshaw, M. W., Pfaff, M., Forsyth, J., Keivens, V. M., Schwartz, M. A., and Ginsberg, M. H. (1997) *Cell* **88**, 521-530

84. Sethi, T., Ginsberg, M. H., Downward, J., and Hughes, P. E. (1999) *Mol Biol Cell* **10**, 1799-1809

85. Zhang, Z., Vuori, K., Wang, H., Reed, J. C., and Ruoslahti, E. (1996) *Cell* **85**, 61-69

86. Han, J., Lim, C. J., Watanabe, N., Soriani, A., Ratnikov, B., Calderwood, D. A., Puzon-McLaughlin, W., Lafuente, E. M., Boussiotis, V. A., Shattil, S. J., and Ginsberg, M. H. (2006) *Curr Biol* **16**, 1796-1806

87. Alberts, B., Johnson, A., Lewis, J., Raff, M., Roberts, K., and Walter, P. (2002) Cell Junctions, Cell Adhesion, and the Extracellular Matrix. In. *Molecular Biology of the Cell*, 4th Edition Ed., Garland Science, New York, NY

88. Katagiri, K., Hattori, M., Minato, N., Irie, S., Takatsu, K., and Kinashi, T. (2000) *Mol Cell Biol* **20**, 1956-1969

89. Bos, J. L. (2005) *Curr Opin Cell Biol* **17**, 123-128

90. Pasvolsky, R., Feigelson, S. W., Kilic, S. S., Simon, A. J., Tal-Lapidot, G., Grabovsky, V., Crittenden, J. R., Amariglio, N., Safran, M., Graybiel, A. M., Rechavi, G., Ben-Dor, S., Etzioni, A., and Alon, R. (2007) *J Exp Med* **204**, 1571-1582

91. Bergmeier, W., Goerge, T., Wang, H. W., Crittenden, J. R., Baldwin, A. C., Cifuni, S. M., Housman, D. E., Graybiel, A. M., and Wagner, D. D. (2007) *J Clin Invest* **117**, 1699-1707

92. Lafuente, E. M., van Puijenbroek, A. A., Krause, M., Carman, C. V., Freeman, G. J., Berezovskaya, A., Constantine, E., Springer, T. A., Gertler, F. B., and Boussiotis, V. A. (2004) *Dev Cell* **7**, 585-595

93. Simonson, W. T., Franco, S. J., and Huttenlocher, A. (2006) *J Immunol* **177**, 7707-7714

94. Calderwood, D. A., Yan, B., de Pereda, J. M., Alvarez, B. G., Fujioka, Y., Liddington, R. C., and Ginsberg, M. H. (2002) *J Biol Chem* **277**, 21749-21758

95. Calderwood, D. A., Zent, R., Grant, R., Rees, D. J., Hynes, R. O., and Ginsberg, M. H. (1999) *J Biol Chem* **274**, 28071-28074

96. Nieswandt, B., Moser, M., Pleines, I., Varga-Szabo, D., Monkley, S., Critchley, D., and Fassler, R. (2007) *J Exp Med* **204**, 3113-3118

97. Petrich, B. G., Fogelstrand, P., Partridge, A. W., Yousefi, N., Ablooglu, A. J., Shattil, S. J., and Ginsberg, M. H. (2007) *J Clin Invest* **117**, 2250-2259

98. Petrich, B. G., Marchese, P., Ruggeri, Z. M., Spiess, S., Weichert, R. A., Ye, F., Tiedt, R., Skoda, R. C., Monkley, S. J., Critchley, D. R., and Ginsberg, M. H. (2007) *J Exp Med* **204**, 3103-3111

99. Ye, F., Hu, G., Taylor, D., Ratnikov, B., Bobkov, A. A., McLean, M. A., Sligar, S. G., Taylor, K. A., and Ginsberg, M. H. (2010) *J Cell Biol* **188**, 157-173

100. Burridge, K., and Connell, L. (1983) *J Cell Biol* **97**, 359-367

101. Burridge, K., and Connell, L. (1983) *Cell Motil* **3**, 405-417

102. Critchley, D. R. (2000) *Curr Opin Cell Biol* **12**, 133-139

103. Critchley, D. R. (2005) *Biochem Soc Trans* **33**, 1308-1312

104. Senetar, M. A., Moncman, C. L., and McCann, R. O. (2007) *Cell Motil Cytoskeleton* **64**, 157-173

105. Rees, D. J., Ades, S. E., Singer, S. J., and Hynes, R. O. (1990) *Nature* **347**, 685-689

106. Pearson, M. A., Reczek, D., Bretscher, A., and Karplus, P. A. (2000) *Cell* **101**, 259-270

107. Elliott, P. R., Goult, B. T., Kopp, P. M., Bate, N., Grossmann, J. G., Roberts, G. C., Critchley, D. R., and Barsukov, I. L. (2010) *Structure* **18**, 1289-1299

108. Schlessinger, J., and Lemmon, M. A. (2003) *Sci STKE* **2003**, RE12

109. Garcia-Alvarez, B., de Pereda, J. M., Calderwood, D. A., Ulmer, T. S., Critchley, D., Campbell, I. D., Ginsberg, M. H., and Liddington, R. C. (2003) *Mol Cell* **11**, 49-58

110. Ulmer, T. S., Calderwood, D. A., Ginsberg, M. H., and Campbell, I. D. (2003) *Biochemistry* **42**, 8307-8312

111. Bouaouina, M., Lad, Y., and Calderwood, D. A. (2007) *J Biol Chem*

112. Anthis, N. J., Wegener, K. L., Ye, F., Kim, C., Goult, B. T., Lowe, E. D., Vakonakis, I., Bate, N., Critchley, D. R., Ginsberg, M. H., and Campbell, I. D. (2009) *Embo J* **28**, 3623-3632

113. Goult, B. T., Bouaouina, M., Elliott, P. R., Bate, N., Patel, B., Gingras, A. R., Grossmann, J. G., Roberts, G. C., Calderwood, D. A., Critchley, D. R., and Barsukov, I. L. (2010) *Embo J* **29**, 1069-1080

114. Wegener, K. L., and Campbell, I. D. (2008) *Mol Membr Biol* **25**, 376-387

115. Vinogradova, O., Vaynberg, J., Kong, X., Haas, T. A., Plow, E. F., and Qin, J. (2004) *Proc Natl Acad Sci U S A* **101**, 4094-4099

116. Lee, H. S., Lim, C. J., Puzon-McLaughlin, W., Shattil, S. J., and Ginsberg, M. H. (2009) *J Biol Chem* **284**, 5119-5127

117. Watanabe, N., Bodin, L., Pandey, M., Krause, M., Coughlin, S., Boussiotis, V. A., Ginsberg, M. H., and Shattil, S. J. (2008) *J Cell Biol* **181**, 1211-1222

118. Ussar, S., Wang, H. V., Linder, S., Fassler, R., and Moser, M. (2006) *Exp Cell Res* **312**, 3142-3151

119. Bialkowska, K., Ma, Y. Q., Bledzka, K., Sossey-Alaoui, K., Izem, L., Zhang, X., Malinin, N., Qin, J., Byzova, T., and Plow, E. F. (2010) *J Biol Chem* **285**, 18640-18649

120. Kloeker, S., Major, M. B., Calderwood, D. A., Ginsberg, M. H., Jones, D. A., and Beckerle, M. C. (2004) *J Biol Chem* **279**, 6824-6833

121. Shi, X., Ma, Y. Q., Tu, Y., Chen, K., Wu, S., Fukuda, K., Qin, J., Plow, E. F., and Wu, C. (2007) *J Biol Chem* **282**, 20455-20466

122. Moser, M., Nieswandt, B., Ussar, S., Pozgajova, M., and Fassler, R. (2008) *Nat Med* **14**, 325-330

123. Ma, Y. Q., Qin, J., Wu, C., and Plow, E. F. (2008) *J Cell Biol* **181**, 439-446

124. Harburger, D. S., Bouaouina, M., and Calderwood, D. A. (2009) *J Biol Chem* **284**, 11485-11497

125. Ussar, S., Moser, M., Widmaier, M., Rognoni, E., Harrer, C., Genzel-Boroviczeny, O., and Fassler, R. (2008) *PLoS Genet* **4**, e1000289

126. Montanez, E., Ussar, S., Schifferer, M., Bosl, M., Zent, R., Moser, M., and Fassler, R. (2008) *Genes Dev* **22**, 1325-1330

127. Moser, M., Bauer, M., Schmid, S., Ruppert, R., Schmidt, S., Sixt, M., Wang, H. V., Sperandio, M., and Fassler, R. (2009) *Nat Med* **15**, 300-305

128. Martel, V., Racaud-Sultan, C., Dupe, S., Marie, C., Paulhe, F., Galmiche, A., Block, M. R., and Albiges-Rizo, C. (2001) *J Biol Chem* **276**, 21217-21227

129. Yan, B., Calderwood, D. A., Yaspan, B., and Ginsberg, M. H. (2001) *J Biol Chem* **276**, 28164-28170

130. Beckerle, M. C., Miller, D. E., Bertagnolli, M. E., and Locke, S. J. (1989) *J Cell Biol* **109**, 3333-3346

131. Nakamura, F., Huang, L., Pestonjamasp, K., Luna, E. J., and Furthmayr, H. (1999) *Mol Biol Cell* **10**, 2669-2685

132. Pufall, M. A., and Graves, B. J. (2002) *Annu Rev Cell Dev Biol* **18**, 421-462

133. Goksoy, E., Ma, Y. Q., Wang, X., Kong, X., Perera, D., Plow, E. F., and Qin, J. (2008) *Mol Cell* **31**, 124-133

134. Goult, B. T., Bate, N., Anthis, N. J., Wegener, K. L., Gingras, A. R., Patel, B., Barsukov, I. L., Campbell, I. D., Roberts, G. C., and Critchley, D. R. (2009) *J Biol Chem* **284**, 15097-15106

135. Franco, S. J., Rodgers, M. A., Perrin, B. J., Han, J., Bennin, D. A., Critchley, D. R., and Huttenlocher, A. (2004) *Nat Cell Biol* **6**, 977-983

136. Ling, K., Doughman, R. L., Iyer, V. V., Firestone, A. J., Bairstow, S. F., Mosher, D. F., Schaller, M. D., and Anderson, R. A. (2003) *J Cell Biol* **163**, 1339-1349

137. Datta, A., Huber, F., and Boettiger, D. (2002) *J Biol Chem* **277**, 3943-3949

138. Johansson, M. W., Larsson, E., Luning, B., Pasquale, E. B., and Ruoslahti, E. (1994) *J Cell Biol* **126**, 1299-1309

139. Campbell, I. D., and Ginsberg, M. H. (2004) *Trends Biochem Sci* **29**, 429-435

140. Shattil, S. J., Hoxie, J. A., Cunningham, M., and Brass, L. F. (1985) *J Biol Chem* **260**, 11107-11114

141. Phillips, D. R., and Scarborough, R. M. (1997) *Am J Cardiol* **80**, 11B-20B

142. Tcheng, J. E., Harrington, R. A., Kottke-Marchant, K., Kleiman, N. S., Ellis, S. G., Kereiakes, D. J., Mick, M. J., Navetta, F. I., Smith, J. E., Worley, S. J., and et al. (1995) *Circulation* **91**, 2151-2157

143. Newman, P. J., Allen, R. W., Kahn, R. A., and Kunicki, T. J. (1985) *Blood* **65**, 227-232

144. Du, X., Saido, T. C., Tsubuki, S., Indig, F. E., Williams, M. J., and Ginsberg, M. H. (1995) *J Biol Chem* **270**, 26146-26151

145. Humphries, J. D., Byron, A., Bass, M. D., Craig, S. E., Pinney, J. W., Knight, D., and Humphries, M. J. (2009) *Sci Signal* **2**, ra51

146. Wishart, D. S., Bigam, C. G., Yao, J., Abildgaard, F., Dyson, H. J., Oldfield, E., Markley, J. L., and Sykes, B. D. (1995) *J Biomol NMR* **6**, 135-140

147. Vranken, W. F., Boucher, W., Stevens, T. J., Fogh, R. H., Pajon, A., Llinas, M., Ulrich, E. L., Markley, J. L., Ionides, J., and Laue, E. D. (2005) *Proteins* **59**, 687-696

148. Kalli, A. C., Wegener, K. L., Goult, B. T., Anthis, N. J., Campbell, I. D., and Sansom, M. S. (2010) *Structure* **18**, 1280-1288

149. Bertagnolli, M. E., Locke, S. J., Hensler, M. E., Bray, P. F., and Beckerle, M. C. (1993) *J Cell Sci* **106 (Pt 4)**, 1189-1199

150. Fillingham, I., Gingras, A. R., Papagrigoriou, E., Patel, B., Emsley, J., Critchley, D. R., Roberts, G. C., and Barsukov, I. L. (2005) *Structure* **13**, 65-74

151. Patel, B., Gingras, A. R., Bobkov, A. A., Fujimoto, L. M., Zhang, M., Liddington, R. C., Mazzeo, D., Emsley, J., Roberts, G. C., Barsukov, I. L., and Critchley, D. R. (2006) *J Biol Chem* **281**, 7458-7467

152. Arias-Salgado, E. G., Lizano, S., Sarkar, S., Brugge, J. S., Ginsberg, M. H., and Shattil, S. J. (2003) *Proc Natl Acad Sci U S A* **100**, 13298-13302

153. Pfaff, M., Liu, S., Erle, D. J., and Ginsberg, M. H. (1998) *J Biol Chem* **273**, 6104-6109

154. Papagrigoriou, E., Gingras, A. R., Barsukov, I. L., Bate, N., Fillingham, I. J., Patel, B., Frank, R., Ziegler, W. H., Roberts, G. C., Critchley, D. R., and Emsley, J. (2004) *Embo J* **23**, 2942-2951

155. Ratnikov, B., Ptak, C., Han, J., Shabanowitz, J., Hunt, D. F., and Ginsberg, M. H. (2005) *J Cell Sci* **118**, 4921-4923

156. Fehon, R. G., McClatchey, A. I., and Bretscher, A. (2010) *Nat Rev Mol Cell Biol* **11**, 276-287

157. Fievet, B. T., Gautreau, A., Roy, C., Del Maestro, L., Mangeat, P., Louvard, D., and Arpin, M. (2004) *J Cell Biol* **164**, 653-659

158. Nakamura, F., Amieva, M. R., and Furthmayr, H. (1995) *J Biol Chem* **270**, 31377-31385

159. Lim, W. A. (2002) *Curr Opin Struct Biol* **12**, 61-68

160. Senetar, M. A., Foster, S. J., and McCann, R. O. (2004) *Biochemistry* **43**, 15418-15428